

Review

Recent Research Progress on All-Solid-State Mg Batteries

Jayaraman Pandeeswari, Gunamony Jenisha, Kumlachew Zelalem Walle  and Masashi Kotobuki * 

Battery Research Center of Green Energy, Ming Chi University of Technology, 84 Gungjuan Rd., Taishan Dist., New Taipei City 24301, Taiwan; pandeesj@gmail.com (J.P.); jenishagunamony@gmail.com (G.J.); kzeybelay1@gmail.com (K.Z.W.)

* Correspondence: kotobuki@mail.mcut.edu.tw

Abstract: Current Li battery technology employs graphite anode and flammable organic liquid electrolytes. Thus, the current Li battery is always facing the problems of low energy density and safety. Additionally, the sustainable supply of Li due to the scarce abundance of Li sources is another problem. An all-solid-state Mg battery is expected to solve the problems owing to non-flammable solid-state electrolytes, high capacity/safety of divalent Mg metal anode and high abundance of Mg sources; therefore, solid-state electrolytes and all-solid-state Mg batteries have been researched intensively last two decades. However, the realization of all-solid-state Mg batteries is still far off. In this article, we review the recent research progress on all-solid-state Mg batteries so that researchers can pursue recent research trends of an all-solid-state Mg battery. At first, the solid-state electrolyte research is described briefly in the categories of inorganic, organic and inorganic/organic composite electrolytes. After that, the recent research progress of all-solid-state Mg batteries is summarized and analyzed. To help readers, we tabulate electrode materials, experimental conditions and performances of an all-solid-state Mg battery so that the readers can find the necessary information at a glance. In the last, challenges to realize the all-solid-state Mg batteries are visited.

Keywords: magnesium battery; solid electrolyte; ceramic electrolyte; polymer electrolyte; all-solid-state Mg battery



Citation: Pandeeswari, J.; Jenisha, G.; Walle, K.Z.; Kotobuki, M. Recent Research Progress on All-Solid-State Mg Batteries. *Batteries* **2023**, *9*, 570. <https://doi.org/10.3390/batteries9120570>

Academic Editor: Seung-Wan Song

Received: 2 October 2023

Revised: 16 November 2023

Accepted: 22 November 2023

Published: 27 November 2023



Copyright: © 2023 by the authors. Licensee MDPI, Basel, Switzerland. This article is an open access article distributed under the terms and conditions of the Creative Commons Attribution (CC BY) license (<https://creativecommons.org/licenses/by/4.0/>).

1. Introduction

Since the Li-ion battery (LIB) was commercialized in 1991, its application in portable electronic devices, such as laptop computers and mobile phones, has been widely achieved, significantly affecting our daily lives [1,2]. As the most successful battery technology, LIBs possess several advantages, including high energy density, no memory effect, good capacity retention, etc., overcoming the last generation lead-acid and nickel–hydrogen batteries [3,4]. Current LIBs rely on the intercalation mechanism. The energy density of LIBs has reached 240 Wh kg^{-1} and 670 Wh L^{-1} at the cell level due to the innovation and development of materials and cell design in these two decades [5,6]. However, the inherent limitation in the theoretical capacity of current graphite-based anodes makes it almost impossible for LIBs to meet the increasing demand for energy density [7]. Li metal anode is an ideal anode material due to its ultimate high theoretical capacity (Table 1), which can improve the energy density of the batteries. Typically, Li-LMO cells (LMO means Li transition metal oxides) have revealed a high energy density of $\sim 440 \text{ Wh kg}^{-1}$ [8]. However, the dendric growth of Li metal and the scarce abundance of Li sources have hindered the commercialization of the Li metal anode.

Solid-state electrolytes, which are solid-state ion conductors, can suppress dendrite growth due to their high mechanical strength [9]. In addition, their inflammable nature and wide electrochemical window can improve the safety and energy density of LIBs. Therefore, solid-state electrolytes and all-solid-state Li batteries have been researched intensively, especially in the last decade [10]. Regarding the low abundance of Li, it is considered that high-abundance elements, such as Na, K, Mg, Ca, Zn and Al, are employed

as charge carriers instead of Li. Particularly, metal anodes of multivalent ions (Mg^{2+} , Ca^{2+} , Zn^{2+} , Al^{3+}) possess higher volumetric capacities than a monovalent Li metal anode. Table 1 summarizes the representative properties of metal anodes. As anode materials, a low redox potential and high specific capacity are desired to achieve the high energy density of batteries. Additionally, a small ionic radius ensures fast ion migration, leading to a high-power density. Mg is in high abundance in the earth's crust and has a high volumetric capacity and a relatively low redox potential. Mg metal was believed to not form the dendrite. Even though a Mg dendrite formation was found in 2017 [11], Mg metal is less prone to the dendrite formation compared to Li and other metals, which has been verified in both experimental and theoretical studies [12,13]. The self-diffusion barrier of Mg is lower than that of Li, which leads to a uniform Mg metal deposition and tends to low dendrite formation. These features make Mg metal an ideal anode material. Therefore, research on an all-solid-state Mg battery and Mg^{2+} -ion conductive solid-state electrolytes has been intensively carried out recently [14,15]. Usually, the research on solid electrolytes has been conducted by testing their chemical (crystal structure, crystallinity, glass transition temperature, etc.) and electrochemical properties (ionic conductivity, electrochemical window, transference number, etc.). The electrochemical properties are examined using blocking electrodes (Pt, Au, etc.) or metal anodes (Mg metal). Additionally, their compatibility with electrodes is characterized in all-solid-state batteries.

Solid-state electrolytes are categorized into the following three groups: organic, inorganic and organic–inorganic composite [16]. Organic solid-state electrolytes are typically flexible and easy to process for large-scale production. On the contrary, inorganic solid-state electrolytes commonly possess a high ionic conductivity, a high transference number and a wide electrochemical window. The organic–inorganic solid-state electrolytes are proposed and developed to address the defects of organic and inorganic solid-state electrolytes, which can combine the advantages of the flexibility and easy processing of organic solid-state electrolytes and the high conductivity of inorganic solid-state electrolytes [17]. Some good review articles focusing on solid-state electrolytes have been published recently [18,19], while research on all-solid-state Mg batteries has yet to be reviewed.

Therefore, in this review article, we focus on the recent research on all-solid-state Mg batteries, especially in the five years (2018~). At first, solid-state electrolyte research is described briefly in the categories of inorganic, organic and inorganic–organic composite electrolytes. After that, the recent research progress of an all-solid-state Mg battery is summarized and analyzed. To help readers, we tabulate electrode materials, experimental conditions (electrolyte and temperature) and performances (initial capacity and cyclability) of all-solid-state Mg batteries so that the readers can find the necessary information at a glance. Lastly, challenges to realize the all-solid-state Mg batteries are visited.

Table 1. Properties of various metal anodes [20].

	Li	Na	K	Mg	Ca	Zn	Al
Standard redox potential (E vs. SHE)	−3.04	−2.71	−2.93	−2.37	−2.87	−0.76	−1.66
Volumetric capacity (mAh/cm ³)	2062	1128	591	3883	2073	5851	8046
Specific capacity (mAh/g)	3861	1166	685	2205	1337	820	2980
Abundance (%)	0.002	2.7	2.4	2.08	5	0.008	8.2
Ionic radius (Å)	0.76	1.02	1.38	0.72	1.00	0.74	0.535
Relative atomic mass	6.94	22.98	39.1	24.31	40.08	65.39	26.98
Mass to charge	6.94	22.98	39.1	12.16	20.04	32.7	8.99

2. Solid Electrolytes for Mg Battery

2.1. Inorganic Electrolyte

2.1.1. Oxides

Na^+ super ion conductor (NASICON), $\text{Na}_{1+x}\text{Zr}_2\text{P}_{3-x}\text{Si}_x\text{O}_{12}$, is well-known for permitting the fast migration of the Na^+ ion due to the well-ordered three-dimensional network structure [21]. By the successful application of the NASICON structure to a Li^+ ion conductive ceramic electrolyte, such as $\text{LiZr}_2(\text{PO}_4)_3$ [22,23], $\text{Li}_{1+x}\text{Al}_x\text{Ti}_{2-x}(\text{PO}_4)_3$ [24,25] or $\text{Li}_{1+x}\text{Al}_x\text{Ge}_{2-x}(\text{PO}_4)_3$ [26,27], it has been highly interested in developing NASICON-type multivalent ion conductors [28,29]. The oxide-based solid electrolytes are usually prepared via calcination of raw materials followed by sintering.

The first report on NASICON-type Mg^{2+} ion conductors was $\text{MgZr}_4(\text{PO}_4)_6$ (MZP) in 1987 [30]. The ionic conductivity was 2.9×10^{-5} and $6.1 \times 10^{-3} \text{ S cm}^{-1}$ at 400 and 800 °C, respectively. MZP was assigned as the rhombohedral structure first, but later it was ascribed to the monoclinic structure, which is like $\beta\text{-Fe}_2\text{SO}_4$. Nakayama et al. simulated Mg^{2+} migration energy of 0.63 and 0.71 eV in the rhombohedral and monoclinic structures, respectively [31]. Thus, heteroatom doping into the Zr^{4+} site to stabilize the rhombohedral structure has been carried out [32,33]. Contrary, another strategy, the introduction of Hf^{4+} into the Mg^{2+} site has also been attempted [34]. However, all results exhibited too low Mg^{2+} ion conductivity, $\sim 10^{-5} \text{ S cm}^{-1}$, even at 500 °C. Those cannot be applied for an all-solid-state Mg battery operated at ambient temperature. It is noted that some promising results were reported by Mohamed's group. They reported $\sigma = 3.97 \times 10^{-4} \text{ S cm}^{-1}$ at room temperature in $\text{Mg}_{1.05}\text{Zn}_{0.4}\text{Al}_{0.3}\text{Zr}_{1.3}(\text{PO}_4)_3$. However, this material demonstrated almost the same conductivity, $5.82 \times 10^{-4} \text{ S cm}^{-1}$ at 500 °C [35]. The extremely low activation energy of 0.039 eV was about one order of magnitude lower than that of typical Li^+ ion conductive ceramics. They also estimated the Mg^{2+} ion transference number by the Bruce method to 0.84 [33]. This implies that 16% of electric charge is carried by an anion, i.e., oxygen ion. In addition, they measured the electrochemical window of $\text{Mg}_{0.5}\text{Si}_2(\text{PO}_4)_3$ to 3.21 V; however, as shown in Figure 1, it seems the decomposition of electrolyte commences below 2 V [36]. We need to re-check their results.

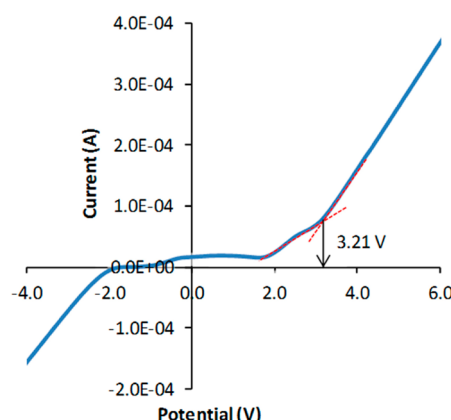


Figure 1. Linear sweep voltammogram of $\text{Mg}_{0.5}\text{Si}_2(\text{PO}_4)_3$. Reproduced with permission [36]. Copyright 2016, Elsevier.

In other research, although magnesium phosphate ($\text{Mg}_{2.4}\text{P}_2\text{O}_{5.4}$) [37], magnesium silicate ($\text{Mg}_{0.6}\text{Al}_{1.2}\text{Si}_{1.8}\text{O}_6$) [38] and magnesium tungstate ($\text{MgHf}(\text{WO}_4)_3$) [39] are researched, a significant improvement of conductivity is still needed. Indeed, all-solid-state Mg batteries using oxide-based solid electrolytes have not been reported yet.

2.1.2. Chalcogenides

Although chalcogenide-based Li^+ ion conductive ceramics like sulfides have succeeded greatly [40], chalcogenide-based Mg^{2+} ion conductive ceramics were not researched intensively. Only one paper was published about the $\text{MgS-P}_2\text{S}_5$ system in 2014 [41]. How-

ever, since Canepa et al. reported trinary spinel chalcogenides with a high Mg^{2+} ion mobility in 2017 [42], research on the chalcogenide-based Mg^{2+} ion conductive ceramics has been activated. They predicted the least migration energy of the Mg^{2+} ion that appeared in MgY_2S_4 , MgY_2Se_4 and $MgSc_2Se_4$, and the values were 360, 361 and 375 meV, respectively (Figure 2); however, only $MgSc_2Se_4$ has been successfully synthesized so far. The Mg^{2+} ion conductivity of $MgSc_2Se_4$ was estimated to be $\sim 1 \times 10^{-4} S\text{ cm}^{-1}$, comparable to Li^{+} ion conductive ceramic electrolytes (garnet-type and NASICON-type) [43]. Unfortunately, electronic conductivity was also relatively high, about $4 \times 10^{-8} S\text{ cm}^{-1}$. Thus, Fichtner et al. synthesized Se-excess, Ti^{4+} , Ce^{4+} -doped $MgSc_2Se_4$ to reduce the electronic conductivity, but the electronic conductivity was not drastically lowered [44]. Based on this, they used $MgSc_2Se_4$ as a cathode material for a Mg battery using liquid electrolytes. Kundo et al. studied the electronic conduction mechanism of $MgSc_2Se_4$ and found that the electronic conductive layer was formed on the surface of particles during the ball milling process [45]. In fact, the electronic conductivity was reduced by avoiding the ball milling process. In addition, the ionic and electronic conductivities of $MgSc_2Se_4$ were largely influenced by the sintering process, particularly the cooling process. Indeed, the field-assisted synthesis could sinter $MgSc_2Se_4$ in a very short time, leading to a low electronic conductivity of $\approx 10^{-11} S\text{ cm}^{-1}$ [46]. Lowering the electronic conductivity of $MgSc_2Se_4$ is a critical issue to apply for all-solid-state Mg batteries. Advanced sintering techniques, which can provide rapid heating/cooling rates and short heat treatments, such as spark plasma sintering (SPS) [23], flash sintering [47], microwave sintering [48] and ultrafast high-temperature sintering [49], should be applied for sintering $MgSc_2Se_4$.

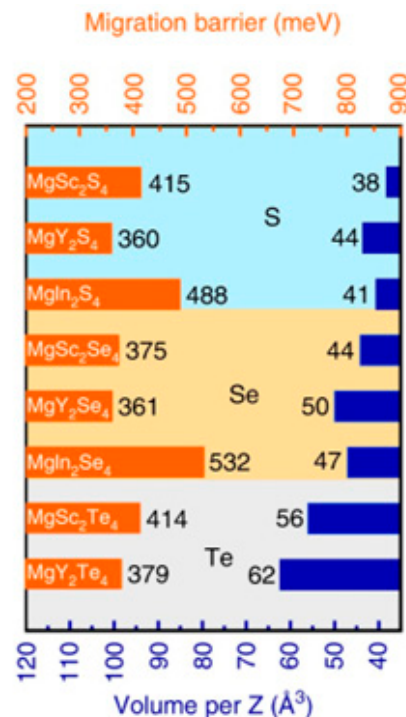


Figure 2. Computed Mg^{2+} ion migration barrier in trinary spinel chalcogenides. Reproduced with permission [42]. Copyright 2017, Nature Communications.

The electrochemical window of $MgSc_2Se_4$ has not been studied yet, but $Au/MgSc_2Se_4/Au$ cell was stable during 3 V of applied voltage [46]. Therefore, $MgSc_2Se_4$ would possess a reasonable electrochemical window for all-solid-state Mg battery application.

The development of $MgSc_2Se_4$ has the following two directions: electrolytes and electrodes. The electronic conductivity of $MgSc_2Se_4$ must be lowered for electrolytes while it is maintained for electrodes. The all-solid-state Mg battery composed of $MgSc_2Se_4$ -based electrodes and $MgSc_2Se_4$ -based electrolytes should have an intimate electrode/electrolyte

interface due to the similar chemical composition and structure, resulting in high and stable performances.

Properties of oxide- and chalcogenide-based electrolytes are summarized in Table 2.

Table 2. Properties of various oxide- and chalcogenide-based solid electrolytes.

Electrolyte	σ_{total} (S cm ⁻¹)	Temperature (°C)	Activation Energy (eV)	Electrochemical Window (V)	Ref.
Oxides					
MgZr ₄ (PO ₄) ₆	2.9×10^{-5}	400	0.868	-	[30]
	6.1×10^{-3}	800			
Mg _{0.5} Zr ₂ (PO ₄) ₃	1.1×10^{-6}	30	0.0977	~ 2.5	[50]
	7.1×10^{-5}	500			
MgZr ₄ (PO ₄) ₆	7.23×10^{-3}	725	0.84	-	[51]
MgZr ₄ (PO ₄) ₆ + Zr ₂ O(PO ₄) ₂	6.9×10^{-3}	800	1.41	-	[52]
Mg _{0.7} (Zr _{0.85} Nb _{0.15}) ₄ (PO ₄) ₆	5.71×10^{-3}	800	0.95	-	
Mg _{1.4} Zr ₄ P ₆ O _{24.4} + 0.4Zr ₂ O(PO ₄) ₂	6.89×10^{-3}	800	1.41	-	[32]
Mg _{1.1} (Zr _{0.85} Nb _{0.15}) ₄ P ₆ O ₂₄ + 0.4Zr ₂ O(PO ₄) ₂	9.53×10^{-3}	800	1.28	-	
Mg _{1.1} Zr _{3.4} Nb _{0.6} P ₆ O _{24.4} + Zr ₂ O(PO ₄) ₂	9.53×10^{-3}	800	1.26	-	[53]
Mg _{0.9} Zr _{1.2} Fe _{0.8} (PO ₄) ₃	1.25×10^{-5}	RT	0.14	-	[33]
	7.2×10^{-5}	500			
Mg _{0.5} Ce _{0.2} Zr _{1.8} (PO ₄) ₃	3.8×10^{-7}	200	0.307	-	[54]
Mg _{1.05} Zn _{0.4} Al _{0.3} Zr _{1.3} (PO ₄) ₃	3.97×10^{-4}	RT	0.039	-	[35]
	5.82×10^{-4}	500			
Mg _{0.35} (Zr _{0.85} Nb _{0.15}) ₂ (PO ₄) ₃	1.1×10^{-6}	350	1.18	-	[55]
Mg _{0.5} ZrSn(PO ₄) ₃	2.47×10^{-5}	500	0.79	-	[56]
Mg _{0.7} Zr _{3.4} Nb _{0.6} (PO ₄) ₆	7.7×10^{-4}	600	0.954	-	[57]
	3.7×10^{-3}	750			
Mg _{0.6} Zr _{1.8} Fe _{0.2} (PO ₄) ₃ thin film	1.8×10^{-7}	25	0.141 < 175 °C 0.511 > 175 °C	-	[58]
	2.3×10^{-6}	200			
Mg _{0.625} Si _{1.75} Al _{0.25} (PO ₄) ₃	1.54×10^{-4}	RT	-	2.51	[59]
Mg _{0.5} Si ₂ (PO ₄) ₃	1.83×10^{-5}	-		~ 3.21	[36]
Mg _{0.105} Hf _{0.95} Nb(PO ₄) ₃	1.2×10^{-4}	600	0.639	-	[34]
Mg _{2.4} P ₂ O _{5.4} ALD	1.6×10^{-7}	500	1.37	-	[37]
Mg _{0.6} Al _{1.2} Si _{1.8} O ₆	2.3×10^{-6}	500	1.32	-	[38]
MgSO ₄ -Mg(NO ₃) ₂ -MgO	2.2×10^{-6}	RT	0.17	-	[60]
MgHf(WO ₄) ₃	2.5×10^{-4}	600	0.835	-	[39]
Chalcogenides					
80(0.6MgS 0.4P ₂ S ₅) 20MgI ₂	2.1×10^{-7}	200	-	-	[41]
MgSc ₂ Se ₄	9.2×10^{-5}	RT	-	-	[44]
MgSc ₂ Se ₄	$\sim 1 \times 10^{-4}$	25	0.38		[42]
MgSc ₂ Se ₄	8×10^{-5}	RT	-	-	[45]
MgSc ₂ Se ₄	1.78×10^{-5}	RT	-	-	[46]

2.1.3. Hydrides

In 2012, Matsuo et al. reported possible Mg conduction in $\text{Mg}(\text{BH}_4)_2$ based on an FPMD simulation [61]. Later, Higashi et al. experimentally proved Mg ion conduction of $\text{Mg}(\text{BH}_4)_2$ and $\text{Mg}(\text{BH}_4)(\text{NH}_2)$ [62]. Since then, $\text{Mg}(\text{BH}_4)_2$ -based electrolytes have been researched the most intensively among the inorganic solid electrolytes. The $\text{Mg}(\text{BH}_4)_2$ -based solid electrolytes are usually prepared by mechanical milling without sintering. Also, an all-solid-state Mg battery with inorganic electrolytes has been fabricated by using only $\text{Mg}(\text{BH}_4)_2$ -based electrolytes (Chapter 3.1). Although the ionic conductivity of $\text{Mg}(\text{BH}_4)(\text{NH}_2)$ is $1 \times 10^{-6} \text{ S cm}^{-1}$ at 150°C [62], it is influenced by the synthetic parameter, for example, the ionic conductivity of $3 \times 10^{-6} \text{ S cm}^{-1}$ at 100°C was obtained in a glass-ceramic like $\text{Mg}(\text{NH}_4)(\text{NH}_2)$ [63]. As other strategies, the modification of BH_4 ligands [64,65], partial oxidation [66], compositing with ceramic oxides such as MgO , YSZ, TiO_2 and Al_2O_3 [67–70] have been attempted, and all achieved an improvement of Mg ion conductivity to $10^{-5}\text{--}10^{-6} \text{ S cm}^{-1}$ at ambient temperature, which is slightly lower than those of Li and Na ion conductive inorganic solid electrolytes [10]. Additionally, they exhibited a stable Mg plating/stripping behavior (Figure 3). However, the modification narrowed the electrochemical window to about $1.2\text{--}1.4 \text{ V}$. This restricts the choice of cathode materials and decreases the energy density of all-solid-state Mg batteries. Although the moderate ionic conductivity and stability against the Mg metal anode of $\text{Mg}(\text{BH}_4)(\text{NH}_2)$ -based inorganic solid electrolytes are desirable, the improvement of anodic stability must be considered. Properties of hydride-based electrolytes are summarized in Table 3.

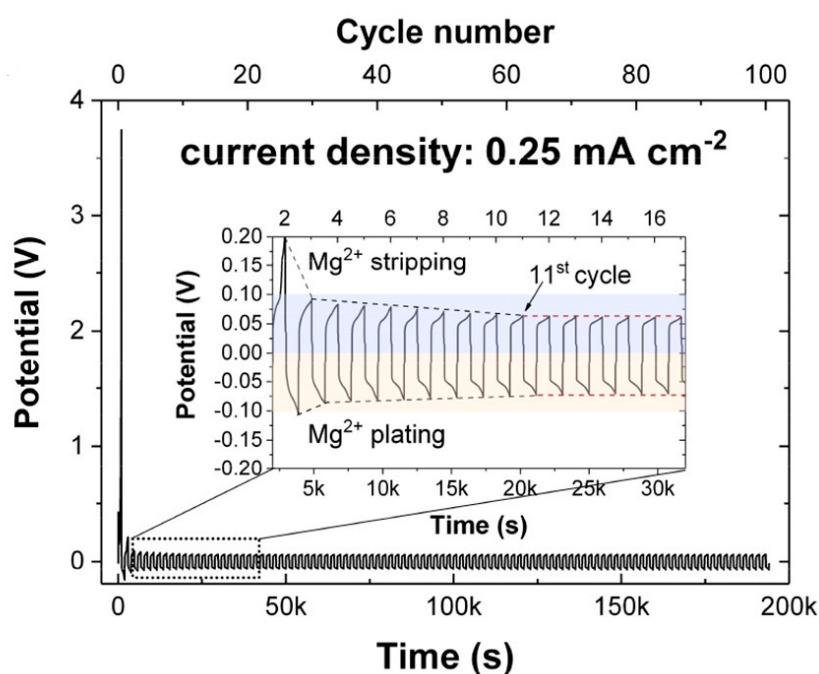


Figure 3. Galvanostatic cycling of a symmetric $\text{Mg}/\text{Mg}(\text{BH}_4)_2 \cdot 1.6\text{NH}_3\text{-MgO}$ cell at 60°C with a constant current density of 0.25 mA cm^{-2} . Reproduced with permission [69]. Copyright 2020, American Chemical Society.

Table 3. Properties of hydride-based solid electrolytes.

Electrolyte	σ_{total} (S cm^{-1})	Temperature ($^\circ\text{C}$)	Activation Energy (eV)	Electrochemical Window (V)	Ref.
$\text{Mg}(\text{BH}_4)_2$	1×10^{-9}	150	-	-	[62]
$\text{Mg}(\text{BH}_4)(\text{NH}_2)$	1×10^{-6}	150	-	3	

Table 3. Cont.

Electrolyte	σ_{total} (S cm^{-1})	Temperature ($^{\circ}\text{C}$)	Activation Energy (eV)	Electrochemical Window (V)	Ref.
Mg(en) ₁ (BH ₄) ₂	5×10^{-8}	30	1.6	1.2	[64]
	6×10^{-5}	70			
Mg(BH ₄)(NH ₂) glass ceramics	3×10^{-6}	100	1.3	-	[63]
Mg(BH ₄) ₂ 1.6NH ₃ -75 wt.% MgO	1.2×10^{-5}	RT	1.12	1.2	[69]
Oxidized Mg(BH ₄) ₂	7.89×10^{-6}	RT	-	-	[66]
Mg(BH ₄) ₂ 1.5THF-75 wt.% MgO	9.8×10^{-7}	30	1.4	1.2	[70]
	1.7×10^{-4}	70			
Mg(BH ₄) ₂ (NH ₃ BH ₃) ₂	1.3×10^{-5}	30	1.47	1.2	[65]
Mg ₃ (BH ₄) ₄ (NH ₂) ₂	4.1×10^{-5}	100	0.84	1.48	[71]
Amorphous Mg(BH ₄) ₂ 2NH ₃	5×10^{-4}	75	1.99	1.4	[72]
Mg(BH ₄) ₂ 1.5NH ₃ -60 wt.% YSZ	3×10^{-4}	50	-	1.3	[67]
Mg(BH ₄) ₂ 1.5NH ₃ -60 wt.% TiO ₂	1.12×10^{-3}	50	0.87	-	
Mg(BH ₄) ₂ 1.6NH ₃ -67 wt.% Al ₂ O ₃	2.5×10^{-5}	22	0.56	1.2	[68]

2.1.4. MOF (Metal–Organic Framework)

MOFs are crystalline solids composed of metal ions coordinated by multifunctional organic molecules with a three-dimensional porous structure. The composition and structure of MOFs can be easily adjusted via the rational selection of the metal ion and organic molecules [73]. Due to the porous structure, diffusivities of guest ions in the pores would be similar to those in a molten salt state [74]; therefore, MOFs have been studied as ionic conductors. To introduce guest ions, pores of MOFs are filled with liquid electrolytes. Thus, MOF-based solid electrolytes would be categorized into liquid–solid composite electrolytes.

Compared to MOF-based Li⁺ ion conductive electrolytes, the studies on Mg²⁺ ion conductors are still few, only eight papers have been published so far. The conductivity of MOF-based Mg ion conductive electrolytes ranges from 10^{-4} to 10^{-6} S cm⁻¹. Since MOF-based solid electrolytes contain liquid electrolytes, the transference number of Mg²⁺ ions should be studied, as well as their electrochemical window. Only three papers reported those, 0.25~0.49 of transference number and about 3 V vs. Mg/Mg²⁺ of oxidative stability [75–77]. On the contrary, stable Mg plating/stripping behavior was observed in four papers (Figure 4) [75–78]; therefore, a Mg metal anode can be applied for the MOF-based electrolytes. Typically, MOF-based Mg ion conductive electrolytes contain around 45~55 wt.% of solvent, which is comparable to gel-polymer electrolytes [79]; however, their conductivities and mechanical properties are not inversely proportional. Hassen et al. reduced the liquid content in MOFs to around 20 wt.% and reported that ionic conductivity was not primarily affected [75]. Also, the same group found conductivity enhancement by treatment of MOF at 150 °C for 24 h, probably due to the removal of coordinated water.

The MOF-based electrolytes are likely to be stable for a Mg metal anode, a relatively high anodic stability, ~3 V, and a high conductivity, which makes them a good candidate for all-solid-state Mg batteries; however, there are still a lot of unknowns. Particularly, the correlation of the pore structure and the composition of a liquid electrolyte (salt, solvent, and salt concentration) with chemical/electrochemical properties must be clarified. Properties of MOF-based solid electrolytes are summarized in Table 4.

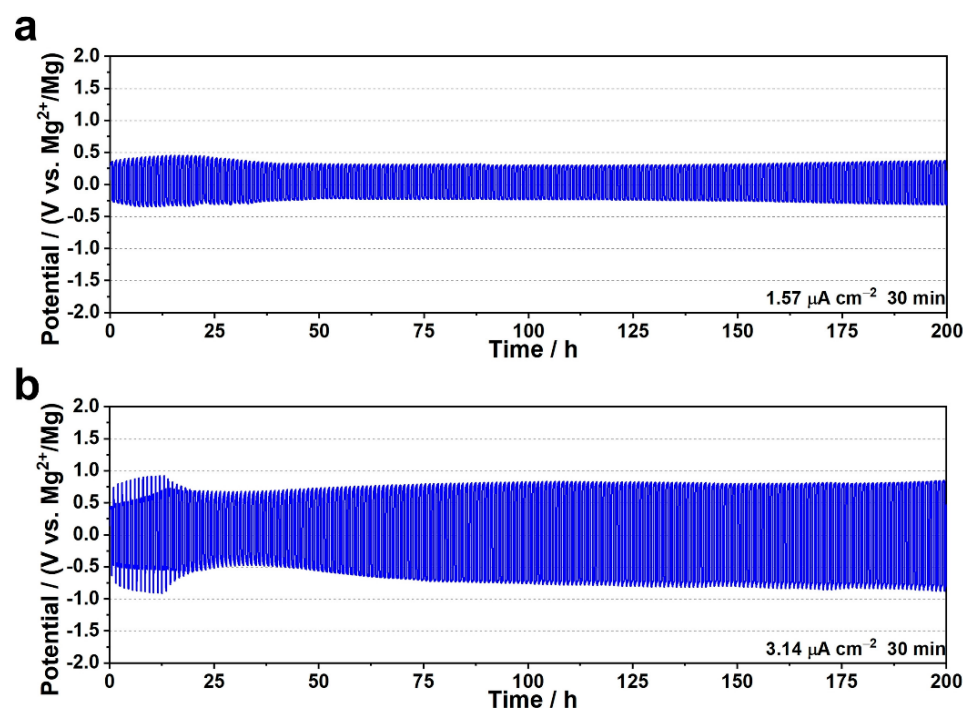


Figure 4. Mg plating/stripping test of UiO-66-Mg(TFSI)₂/[EMIM][TFSI] electrolyte at current density of (a) 1.57 $\mu\text{A cm}^{-2}$ and (b) 3.14 $\mu\text{A cm}^{-2}$ at 60 $^{\circ}\text{C}$. Reproduced with permission [76]. Copyright 2022, Wiley-VCH GmbH.

Table 4. Properties of MOF-based solid electrolytes.

MOF	Liquid Electrolyte	σ_{total} (S cm^{-1})	Temperature ($^{\circ}\text{C}$)	Activation Energy (eV)	Ref.
$\text{Mg}_2(\text{dobpdc})$	Mg(TFSI) ₂ /triglyme	1.3×10^{-4}	RT	0.11~0.19	[79]
	Mg(OPhCF ₃) ₂ + Mg(TFSI) ₂ /triglyme	2.5×10^{-4}	RT		
MIT-20	MgBr ₂ /PC	8.8×10^{-7}	RT	0.37	[80]
$\text{Cu}_4(\text{ttpm})_2 \cdot 0.6\text{CuCl}_2$	MgCl ₂ /THF	1.2×10^{-5}	RT	0.32	[81]
	MgBr ₂ /THF	1.3×10^{-4}	RT	0.24	
MOF-74	Mg(TFSI) ₂ /MgCl ₂ /DME	3.17×10^{-6}	RT	0.53	[78]
Mgbp3dc	α -Mg ₃ (HCOO) ₆ /DMF	3.8×10^{-5}	RT	0.669	[75]
UiO-66	Mg(TFSI) ₂ /[EMIM][TFSI]	5.8×10^{-5}	RT	0.67	[76]
MOF-177	Mg(TFSI) ₂ /diglyme	1.6×10^{-5}	RT	0.33	[77]
MIL-101	Mg(TFSI) ₂ + MeCN vapor	1.9×10^{-3}	25	0.18	[82]

2.2. Organic Electrolyte

Organic electrolytes, namely, polymer electrolytes, are composed of polymer hosts and Mg salts (solid polymer electrolytes, SPEs). In some cases, fillers and plasticizers are added to improve the properties. SPEs have been reported the most, while SPEs with plasticizers are most widely employed for all-solid-state Mg batteries. Herein, recent research on organic electrolytes is briefly summarized. Recently, novel organic electrolytes, i.e., organic crystal electrolytes, have been developed. Organic crystal electrolytes are introduced at the end of this section. For Mg²⁺ ion conductive electrolytes, only inorganic fillers are employed. Therefore, filler-added polymer electrolytes are reviewed in the next Section 2.3 “Organic-inorganic composite electrolytes”.

2.2.1. Solid Polymer Electrolytes

SPEs are composed of host polymers and Mg salts. The Lewis-base moieties of host polymers allow the dissociation of Mg salts, resulting in an emerging Mg^{2+} ion conduction. Accordingly, the host polymers contain atoms with lone-pair electrons, such as oxygen, fluorine and nitrogen atoms. Figure 5 depicts the structures of various host polymers. SPEs are prepared by the solution-casting method. Polymer hosts and Mg salts are dissolved into a solvent and then cast onto a substrate to obtain SPE films.

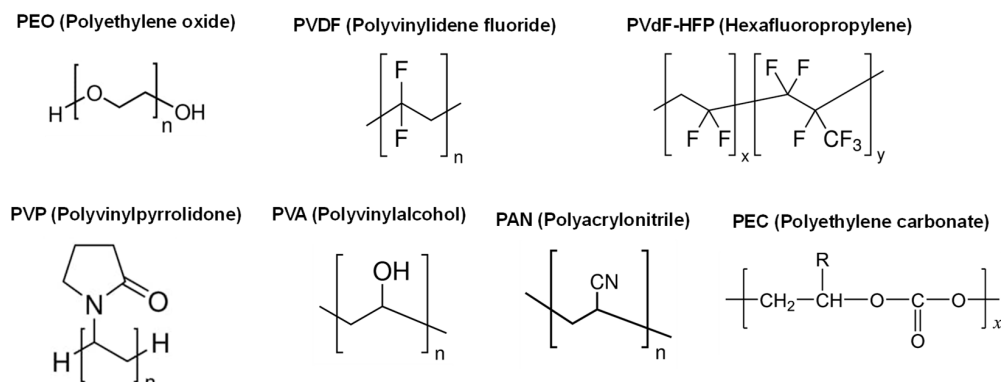


Figure 5. Structures of various host polymers used in Mg^{2+} ion conductive polymer electrolytes.

Common host polymers, such as PEO, have been used in Mg^{2+} -ion conductive SPEs [83,84]. Different from Li^+ ion conductive SPEs, water-soluble polymers like PVP and PVA are also used [85–88]. Such polymers allow the use of water as a solvent, facilitating preparation processes and reducing production costs. The ionic conductivities of SPEs using the water-soluble polymer hosts are comparable ($10^{-5}\sim10^{-6} \text{ S cm}^{-1}$) to the conventional polymer hosts; however, other properties like the electrochemical window are seldom studied. Studies on the other properties must be carried out to clarify the applicability of the water-soluble polymer hosts.

Solvents used for polymer casting would influence the properties of SPEs. Unfortunately, direct research on the influence of solvents has not been performed. Organic and inorganic solvents have been usually employed for synthetic and natural polymers, respectively. A large performance difference by solvents was not confirmed among organic and inorganic solvents.

Natural polymers are also used as host polymers for Mg²⁺ ion conductive SPEs [89–104]. Natural polymers are attractive in terms of environmental friendliness and resource abundance. Natural polymer-based SPEs exhibit better conductivity, around one order of magnitude higher than synthetic polymer-based SPEs. Notably, SPEs composed of potato starch and Gellan gum reveal a high ionic conductivity of ~10⁻² S cm⁻¹ [92], which is comparable to Li₁₀GeP₂S₁₂ and even liquid electrolytes [105]. In addition, these SPEs possess high flexibility and are promising for all-solid-state Mg batteries. However, their application to all-solid-state Mg batteries has yet to be reported. The environmental friendliness of natural polymers means that natural polymers will decompose naturally in the long term. Thus, the long-term stability of natural polymer-based SPEs must be tested.

To improve the properties of SPEs, a polymer blend, namely, a mixture of two host polymers, was also studied [106–116]. By the blending, the ionic conductivity increases by one order of magnitude, $10^{-3}\text{--}10^{-4}$ S cm $^{-1}$, which is applicable to all-solid-state Mg batteries. Recently, the blend of natural and synthetic polymers emerged as a new research trend in SPEs [117–120]. For example, in the blend of methyl cellulose (MC) and PVA, the hydrogen bond forms between MC and PVA, stabilizing the polymer blend [119]. In addition, rich-oxygen atoms in MC facilitate the dissociation of Mg salts. As a result, the ionic conductivity increased to $\sim 10^{-4}$ S cm $^{-1}$, which is applicable to all-solid-state Mg batteries [121].

Regarding the Mg salts, in addition to commonly used metal salts in LIBs like TFSI, ClO_4 -salts, more cost-effective MgSO_4 , $\text{Mg}(\text{NO}_3)_2$, MgCl_2 , etc., are used. Thus, water-soluble polymers, such as PVA and PVP, are used for these salts. The ionic conductivity was not influenced by the Mg salts. Aziz et al. added LiFSI into PEC-Mg(TFSI)₂ SPE [122]. The ionic conductivity was improved by one order of magnitude by the addition. Also, the Li-contained SPE demonstrated stable Mg stripping and plating. The usage of mixing salt is a new concept for the SPEs. In this system, the contribution of Li-ion conduction must be considered to estimate the ionic conductivity. However, characterization techniques to extract only Mg^{2+} ion conduction have not been developed yet; therefore, the characterization of the system should be given extra consideration.

Many types of polymers and Mg salts are studied for Mg^{2+} -ion conductive SPEs. Most studies focus on the ionic conductivity, however, other properties, such as electrochemical window, transference number and compatibility with electrodes, are also important for application of all-solid-state batteries. Thus, studies on SPEs should be performed more comprehensively. Properties of SPEs are summarized in Table 5.

Table 5. Properties of SPEs.

Polymer	Mg Salt	Solvent	σ_{total} (S cm^{-1})	Temp. ($^{\circ}\text{C}$)	E_a (eV)	Window (V vs. Mg/Mg^{2+})	t_+	Ref.
PEO	$\text{Mg}(\text{TFSI})_2$	ACN	1.8×10^{-6}	0	0.68	-	-	[83]
			1.6×10^{-4}	50				
PEO	$\text{Mg}(\text{ClO}_4)_2$	methanol	1.42×10^{-6}	RT	-	-	-	[84]
PVP	MgCl_2	DI water	1.42×10^{-5}	RT	-	-	-	[85]
PVP	MgSO_4	DI water	1.05×10^{-5}	RT	-	-	-	[86]
PVA	MgSO_4	DI water	1×10^{-9}	27	0.37	-	-	[87]
PVA	MgCl_2	DI water	5×10^{-7}	35	-	-	-	[88]
Potato starch	MgCl_2	methanol	3.2×10^{-2}	RT	0.002	4.6	-	[89]
Sodium alginate	$\text{Mg}(\text{NO}_3)_2$	DI water	4.58×10^{-3}	RT	-	3.5	0.31	[90]
MC	$\text{Mg}(\text{NO}_3)_2$	DI water	1.02×10^{-4}	RT	-	3.23	-	[91]
Gellan gum	$\text{Mg}(\text{ClO}_4)_2$	DI water	1.06×10^{-2}	RT	-	2.86	0.33	[92]
Natural rubber	$\text{Mg}(\text{Tf})_2$	THF	4.9×10^{-3}	30	-	2.5	-	[93]
I-Carrageenan	$\text{Mg}(\text{NO}_3)_2$	DI water	6.1×10^{-4}	30	0.17	-	-	[94]
Agarose	$\text{Mg}(\text{NO}_3)_2$	DMSO	1.48×10^{-5}	RT	0.044	3.57	-	[95]
CA	$\text{Mg}(\text{NO}_3)_2$	DMF	9.19×10^{-4}	RT	-	3.65	0.35	[96]
K-Carrageenan	MgCl_2	DI water	4.76×10^{-3}	30	-	1.94	0.26	[97]
Chitosan	$\text{Mg}(\text{Tf})_2$	1% acetic acid aq.	9.58×10^{-5}	RT	0.36	-	-	[98]
K-Carrageenan	$\text{Mg}(\text{NO}_3)_2$	DI water	7.05×10^{-4}	RT	-	4.42	0.32	[99]
Methyl cellulose	$\text{Mg}(\text{CH}_3\text{COO})_2$	DI water	2.6×10^{-5}	RT	-	3.47	-	[100]
I-carrageenan	$\text{Mg}(\text{ClO}_4)_2$	DI water	2.18×10^{-3}	RT	0.05	-	0.313	[101]
Chitosan	MgCl_2	1% acetic acid aq	4.6×10^{-4}	-	-	-	-	[102]
Pectin	$\text{Mg}(\text{NO}_3)_2$	DI water	7.7×10^{-4}	RT	-	3.8	0.29	[103]
Pectin	MgCl_2	DI water	1.14×10^{-3}	RT	-	2.05	0.301	[104]
PEO-PVDF	MgTFSI	DMF	1.2×10^{-5}	25	-	-	-	[105]
PEO/PVDF-HFP	MgBr_2	DMF	3.9×10^{-4}	RT	0.26	1.86	-	[106]
PVA-PAN	$\text{Mg}(\text{ClO}_4)_2$	DMF	2.94×10^{-4}	RT	0.21	3.65	0.27	[107]
PVDF-HFP + PVAc	$\text{Mg}(\text{ClO}_4)_2$	THF	1.60×10^{-5}	30	0.33	3.5	-	[109]
PVP-PVA	$\text{Mg}(\text{NO}_3)_2$	DI water	3.8×10^{-5}	30	0.475	-	-	[110]
PVA-PAN	MgCl_2	DMF	1.01×10^{-3}	RT	0.07	3.66	-	[111]
Poly(VdCl-co-AN-co-MMA)	$\text{Mg}(\text{NO}_3)_2$	THF	1.6×10^{-4}	RT	0.19	3.2	0.36	[112]

Table 5. Cont.

Polymer	Mg Salt	Solvent	σ_{total} (S cm^{-1})	Temp. ($^{\circ}\text{C}$)	E_a (eV)	Window (V vs. Mg/Mg^{2+})	t_f	Ref.
PEO/PO	$\text{Mg}(\text{TFSI})_2$	ACN	1.5×10^{-5}	30	-	-	-	[113]
PCL-PTMC	$\text{Mg}(\text{TFSI})_2$	ACN	2.52×10^{-8}	25	-	-	-	[114]
PVA-PAN	$\text{Mg}(\text{NO}_3)_2$	DMF	1.71×10^{-3}	RT	0.36	3.4	0.30	[115]
PVDF-HFP + PVAc	$\text{Mg}(\text{ClO}_4)_2$	THF	3.85×10^{-5}	30	3.37	3.68	-	[116]
CS + MC	MgCl_2	1% acetic acid aq	2.75×10^{-3}	30	-	3.86	-	[117]
Corn silk + PVA	MgCl_2	DI water	1.28×10^{-3}	RT	-	2.11	0.32	[118]
Methyl cellulose-PVA	$\text{Mg}(\text{NO}_3)_2$	Not mention	3.25×10^{-4}	27	-	2.62	-	[119]
PEO-Starch	MgBr_2	methanol	7.8×10^{-9}	RT	-	-	-	[120]
PEC	$\text{Mg}(\text{TFSI})_2$	ACN	2.3×10^{-6}	80	-	2.0	-	[122]
Polysaccharide	$\text{Mg}(\text{ClO}_4)_2$	DI water	5.66×10^{-4}	RT	0.09	3.93	0.43	[123]
PEC	$\text{Mg}(\text{ClO}_4)_2$	ACN	5.2×10^{-5}	90	-	-	-	[124]
PAGE	$\text{Mg}(\text{TFSI})_2$	THF	4.1×10^{-4}	90	-	-	-	[125]

2.2.2. Polymer Electrolytes with Plasticizers (Gel-Polymer Electrolytes)

In general, plasticizers are used to soften a material, to increase its plasticity and to decrease its viscosity. In polymer electrolytes, plasticizers lower T_g (glass-transition temperature) and activate the segmental motion of polymer chains, enhancing ionic conductivity. Studies on all-solid-state Mg batteries have been performed using GPEs the most.

As Li^{+} -ion conductive polymer electrolytes, low molecular weight solvents and ionic liquids have been used as plasticizers (Figure 6). Because plasticizers soften SPEs, the optimum amount of plasticizers must be found to balance the ionic conductivity and mechanical properties of GPEs. The optimum amount of plasticizers varies significantly by the plasticizers used. In the GPE using $\text{PYR}_{14}\text{TFSI}$ ionic liquid, the highest ionic conductivity was obtained at 10 wt.% of plasticizers [126]. Contrarily, the plasticizer amount of 200 wt.% was reported in the TEGDME system [127]. In such high plasticizer content, it is questioned whether the ionic conduction is mainly caused by the segmental motion of the polymer or dissolved Mg salt in the liquid part.

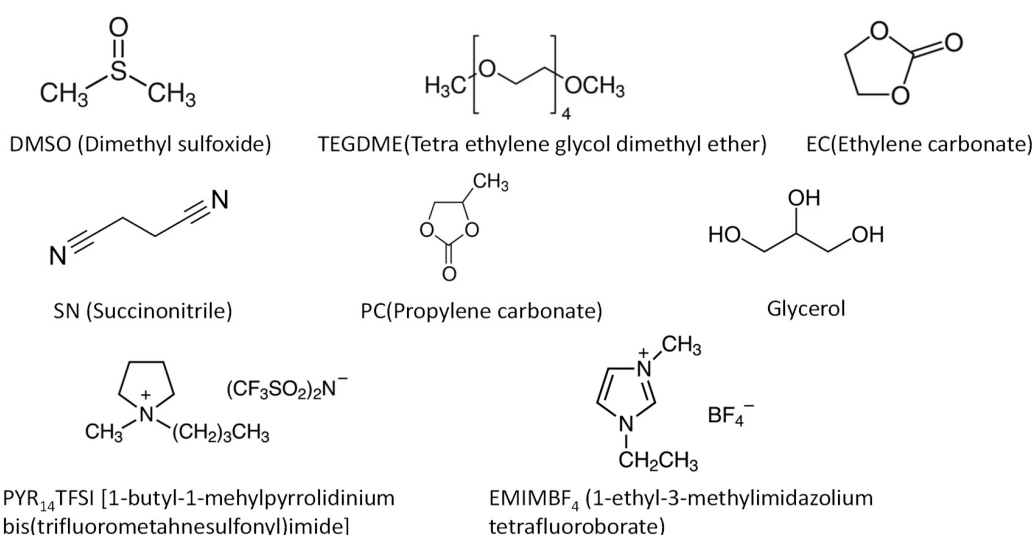


Figure 6. Structures of various plasticizers used in Mg^{2+} ion conductive polymer electrolytes.

In GPEs, synthetic polymers are mostly studied. Their conductivity ranges from 10^{-4} to $10^{-3} \text{ S cm}^{-1}$, which can be applied for all-solid-state batteries. Gupta et.al. reported a high ionic conductivity of $2 \times 10^{-2} \text{ S cm}^{-1}$ in [PVdF-HFP(30 wt.%)–EMIMBr(70 wt.%)]

(30 wt.%)-[PC-Mg(ClO₄)₂ (0.3 M)] (70 wt.%) system [128]. However, cell data were not reported although the high ionic conductivity is promising. Mixed plasticizers like EC-SN [129] and EC-DEC [130] have also been studied, but they did not significantly improve properties compared with single plasticizers.

The inorganic magnesium aluminum chloride complex (MgCl₂-AlCl₃, MACC) has been studied in liquid electrolytes [131]. With the addition of AlCl₃, the dissociation of MgCl₂ is promoted, increasing the solubility of the MgCl₂ and Mg²⁺-ion concentrations. As a result, Mg stripping/plating over potential can be drastically decreased [132]. Wang et al. applied this concept to GPEs for the first time [133]. The ionic conductivity of their PVDF-HFP-based GPEs containing a MgCl₂-AlCl₃ salt and a TEGDME plasticizer was 4.7×10^{-4} S cm⁻¹. Although this value was comparable to other GPEs, the reversibility of Mg stripping/plating was drastically improved. In polymer electrolyte research, the effect of Mg salt has not been studied intensively. Their results clearly show the importance of Mg salt on the performance of all-solid-state Mg batteries.

In another important study, a single-ion conductive polymer electrolyte was reported by Schaefer et al. [134]. In the single-ion conductive polymer electrolyte, the anion part of Mg salt was polymerized with host polymers. Thus, the mobility of the anion is zero; in other words, the cation transference number is 1. Therefore, undesired side reactions caused by anions can be avoided completely. The authors prepared a P(PEGDMA)-P(TFSI) [poly(ethylenglycol) dimethacrylate- poly styrenesulfonyl (trifluoromethylsulfonyl)] network (Figure 7). In this structure, TFSI moiety is involved in the polymer chain, resulting in the immobilization of anion. This type of polymer generally shows a low ionic conductivity due to the low segmental motion of the polymer chain. Thus, the DMSO plasticizer was added, and the Mg²⁺-ion conductivity was increased to 8.8×10^{-4} S cm⁻¹. It is noted that the high conductivity was achieved by only Mg²⁺-ion transportation. Some other studies reported higher conductivities; however, the conductivities contain anion transportation. Therefore, the high Mg²⁺-ion conductivity of single-ion conductive polymer is very attractive. Unfortunately, cell data were not reported.

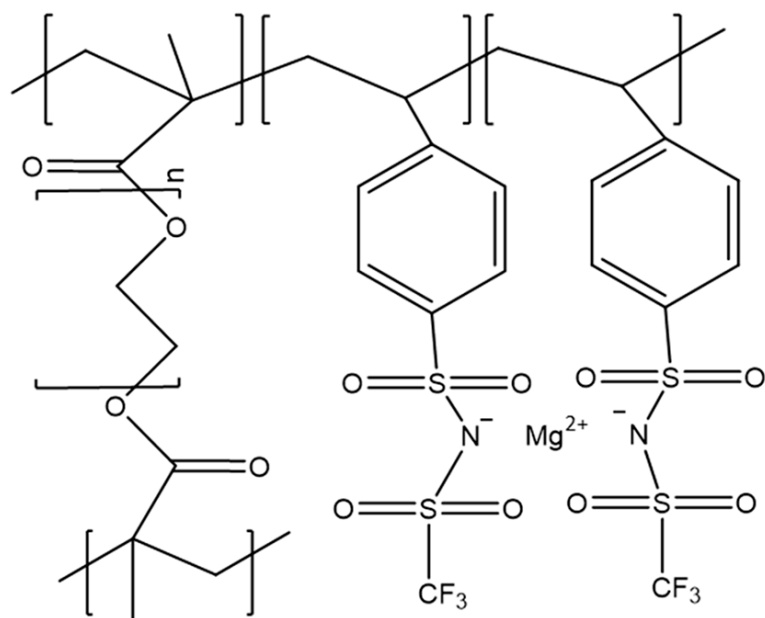


Figure 7. Structures of magnesiated P(PEGDMA)-P(STFSI) network.

In GPEs, mixed salts like MACC and the single-ion conductive polymer are studied. Such studies have been carried out only in GPEs. Their superior properties are promising to apply for all-solid-state Mg batteries. This concept should be investigated intensively and used in other polymer electrolytes, such as organic-inorganic composite electrolytes. Properties of GPEs are summarized in Table 6.

Table 6. Properties of GPEs.

Polymer	Mg Salt	Plasticizer	σ_{total} (S cm ⁻¹)	Temp. (°C)	E _a (eV)	Window (V vs. Mg/Mg ²⁺)	Transference Number	Ref.
P(PEGDMA)-P(STFSI)		DMSO	8.8×10^{-4}	30	-	1.5	(1.0)	[134]
PVDF	Mg(SO ₃ CF ₃) ₂	TEGDME	4.6×10^{-4}	55	0.62	1.0	0.74	[135]
PEO	Mg(Tf) ₂	PYR ₁₄ TFSI	3.7×10^{-4}	RT	-	-	0.40	[126]
PEO	Mg(Tf) ₂	EMIM-BF ₄	9.4×10^{-5}	RT	0.26	4.0	0.22	[136]
PVdC-co-AN	Mg(TFSI) ₂	EC + SN	1.9×10^{-6}	RT	0.04	3.8	0.59	[129]
PVdC-co-AN	Mg(TFSI) ₂	SN	1.6×10^{-6}	RT	0.09	3.2	-	[137]
PVDF-HFP	Mg(ClO ₄) ₂	EDiMIMBF ₄	8.4×10^{-3}	RT	0.33	-	-	[138]
PVDF-HFP	Mg(ClO ₄) ₂	EMIMBr, PC	2.0×10^{-2}	RT	0.02	-	-	[128]
PEC	Mg(TFSI) ₂	TEGDME	5.2×10^{-6}	80	-	-	-	[139]
PECH-OH	MgCl ₂	TEGDME	6.2×10^{-5}	30	0.25	3.2	0.79	[127]
PVDF-HFP	Mg(Tf) ₂	SN + EMITf	4×10^{-3}	26	0.104	4.1	-	[140]
Poly(VdCl-co-An-co-MMA)	MgCl ₂	SN	1.4×10^{-3}	RT	0.26	3.3	0.31	[141]
c-PTHF	Mg(TFSI) ₂	TEGDME	4.5×10^{-5}	30	-	-	-	[142]
CS	Mg(CH ₃ COO) ₂	glycerol	1.1×10^{-4}	RT	-	-	-	[143]
k-carrageenan	Mg(NO ₃) ₂	EC	7.3×10^{-3}	30	-	4.59	0.39	[103]
PVDF-HFP/PVAc	Mg(ClO ₄) ₂	EMITf	9.1×10^{-4}	30	0.28	3.59	-	[144]
Hydroxy propyl	Mg(TFSI) ₂	TEGDME	1.73×10^{-3}	25	-	-	-	[145]
PVDF-HFP	Mg(Tf) ₂	EC-DEC	2.4×10^{-4}	70	-	5.0	0.42	[130]
PVDF	Mg(ClO ₄) ₂	PC	1.5×10^{-3}	RT	-	5.0	0.47	[146]
PVDF-HFP	Mg(ClO ₄) ₂	TEGDME	9.8×10^{-4}	RT	-	4.6	-	[147]
PTHF	MgBOR		2.0×10^{-3}	25	-	2.57	0.3	[148]
PVA	Mg(Tf) ₂	EMITf	1.2×10^{-3}	RT	-	-	-	[149]
PVDF-HFP	Mg(ClO ₄) ₂	PC	1.6×10^{-3}	RT	-	5.5	-	[150]
PAN	Mg(ClO ₄) ₂	PC	3.3×10^{-3}	30	0.1	4.6	0.6	[151]
PVDF-HFP	MgCl ₂ -AlCl ₃	TEGDME	4.7×10^{-4}	25	-	3.1	-	[133]
PEO	Mg(Tf) ₂	PC-DEC	3.0×10^{-5}	RT	0.14	3.5	0.32	[152]
CS:Dextran	Mg(CH ₃ COO) ₂	Glycerol	1.2×10^{-6}	RT	-	1.5	-	[153]

2.2.3. Organic Crystal Electrolytes

Recently, Moriya's group reported a new type of organic electrolyte, organic crystal electrolytes. They are composed of organic molecules and Mg salts and possess ion conduction paths in the crystal lattice (Figure 8). The paths are precisely controlled by organic molecules and Mg salts. Only two Mg ion conductive organic crystal electrolytes have been reported so far [154,155]. In both cases, their room temperature conductivities were higher or comparable to Mg(BH₄)₂-based inorganic electrolytes, and the cation transference number was higher than that of polymer-based electrolytes. These properties would be improved by adjusting the ion conduction paths. Unfortunately, cell data using the organic crystal electrolytes are not available at the moment. There is still a lot of room to develop organic crystal electrolytes. Properties of organic crystals are summarized in Table 7.

Table 7. Properties of organic crystals.

Crystal	σ_{total} (S cm ⁻¹)	Temp. (°C)	E _a (eV)	Transference Number	Ref.
Mg(TFSA) ₂ (CPME) ₂	2×10^{-7}	30	0.72	0.74	[154]
[N ₁₁₂₂][Mg(η^2 -TFSA) ₂ (μ_2 - η^1 - η^1 -TFSA)]	2.5×10^{-6}	40	1.21	0.46	[155]

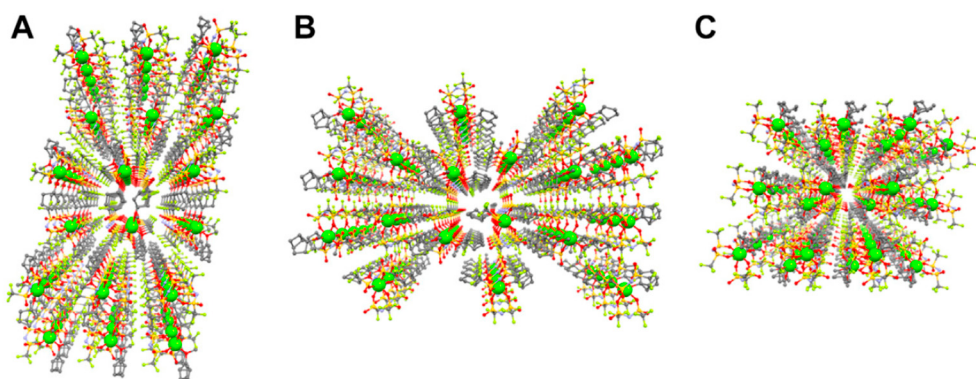


Figure 8. Packing view with ball and stick model of $\text{Mg}(\text{TFSA})_2(\text{CPME})_2$. Mg-ions are emphasized as a large sphere. (A) along the a-axis, (B) along the b-axis, and (C) along the c-axis (Mg: green, C: gray, N: pale blue, O: red, F: pale green, S: dark yellow. H atoms are omitted for clarity). Reproduced with permission [154]. Copyright 2021, Frontiers.

2.3. Organic–Inorganic Composite Electrolytes

2.3.1. Solid Polymer Electrolytes with Fillers

In the Li^+ ion conductive polymer electrolytes, various types of fillers, such as organic/inorganic fillers and active/passive (Li^+ ion conductive/non- Li^+ ion conductive) fillers are researched. Contrarily, in the Mg^{2+} ion conductive polymer electrolytes, only inorganic passive fillers, especially metal oxides, are studied. In addition, only nanoparticle morphology, not nano-wire, nano-sheet, etc., is employed. Among the studies, the highest conductivity was obtained in filler contents of 3~7 wt.% regardless of the fillers. An interesting study was carried out by Jayanthi et al. in which the ferroelectric material, BaTiO_3 , was added to PVDF-HFP/MgTf polymer electrolyte as a filler [156]. The presence of ferroelectric domains in the polymer electrolyte facilitates salt dissociation and helps the amorphization of the polymer, enhancing ionic conductivity. A similar study was reported in Na^+ ion conductive polymer electrolyte [157]. In this case, $\text{K}_{0.5}\text{Na}_{0.5}\text{NbO}_3$ (KNN) was used as a ferroelectric filler, and it decreased the ionic conductivity of polymer electrolytes, while the stability against the Na metal anode was improved. As a result, a better performance of an all-solid-state Na battery was obtained. This is a good result that electrolyte performance is determined by conductivity and interface properties between electrodes and electrolytes. Thus, electrolyte study must include the construction and evaluation of an all-solid-state battery. Unfortunately, studies on only solid electrolytes have been reported much more than all-solid-state batteries. Properties of SPEs with fillers are summarized in Table 8.

Table 8. Properties of SPEs with fillers.

Polymer	Mg Salt	Filler	σ_{total} (S cm^{-1})	Temp. ($^{\circ}\text{C}$)	E_a (eV)	Window (V vs. Mg/Mg^{2+})	Transference Number	Ref.
PVA/PVP	MgCl_2	CuS	4.3×10^{-6}	RT	-	-	-	[158]
MC	MgCl_2	ZnO	1.2×10^{-4}	RT	-	-	-	[159]
PVDF	$\text{Mg}(\text{NO}_3)_2$	MgO	1.0×10^{-4}	RT	0.32	-	-	[160]
PEG	$\text{Mg}(\text{CH}_3\text{COO})_2$	CeO_2	3.4×10^{-6}	RT	-	-	-	[161]
PMMA	$\text{Mg}(\text{Tf})_2$	TiO_2	1.8×10^{-6}	RT	-	-	-	[162]
CS	$\text{Mg}(\text{NO}_3)_2$	MnO_2	1.2×10^{-3}	30	-	1.7	-	[163]
PVDF-HFP	$\text{Mg}(\text{Tf})_2$	BaTiO_3	4.1×10^{-4}	RT	-	-	-	[156]
PEO	$\text{Mg}(\text{Tf})_2$	MgO	1.6×10^{-4}	25	0.14	-	-	[164]
PVDF	$\text{Mg}(\text{NO}_3)_2$	Al_2O_3	9.5×10^{-6}	RT	-	-	-	[165]
PVDF	$\text{Mg}(\text{NO}_3)_2$	ZnO	5.2×10^{-5}	RT	0.29	-	-	[166]

Table 8. Cont.

Polymer	Mg Salt	Filler	σ_{total} (S cm ⁻¹)	Temp. (°C)	E _a (eV)	Window (V vs. Mg/Mg ²⁺)	Transference Number	Ref.
PEO	MgCl ₂	B ₂ O ₃	7.2×10^{-6}	25	-	-	-	[167]
PVDF-HFP/PVAc	Mg(ClO ₄) ₂	MgTiO ₃	5.8×10^{-3}	30	0.25	4.0	0.34	[168]
CS	MgCl ₂	V ₂ O ₅	1.4×10^{-3}	RT	-	1.7	-	[169]
PVDF-HFP	MgClO ₄	ZrO ₂	6.6×10^{-2}	30	-	-	-	[170]
PVDF-HFP	MgCl ₂	ZnO	1.3×10^{-5}	RT	-	-	-	[171]

Table 9. Properties of SPEs with plasticizers and fillers.

Polymer	Mg Salt	Plasticizer	Filler	σ_{total} (S cm ⁻¹)	Temp. (°C)	E _a (eV)	Window (V vs. Mg/Mg ²⁺)	Transference Number	Ref.
CS/MC	Mg(CH ₃ COO) ₂	Glycerol	Ni	1.0×10^{-4}	RT	-	2.48	-	[172]
PEO	Mg(ClO ₄) ₂	EMIMFSI	SiO ₂	5.4×10^{-4}	RT	0.36	4.0	-	[174]
CS	Mg(CH ₃ COO) ₂	Glycerol	Ni	1.1×10^{-5}	RT	-	2.4	-	[175]
PVDF-HFP	Mg(Tf) ₂	EC-PC	MgAl ₂ O ₄	4.0×10^{-3}	RT	-	-	0.66	[173]
PVDF-HFP	Mg(ClO ₄) ₂	PTR ₁₄ RFSI	TiO ₂	1.6×10^{-4}	30	0.13	-	0.23	[176]
PVDF-HFP	Mf(TFSI) ₂	TEGDME	SiO ₂	8.3×10^{-4}	RT	-	-	-	[177]
PTHF	Mg(BH ₄) ₂ ⁻ LiBH ₄	diglyme	TiO ₂	4.2×10^{-4}	40	0.003	-	0.5	[178]

2.3.2. Solid Polymer Electrolytes including Plasticizers and Fillers

In this system, polymer electrolytes contain both inorganic fillers and plasticizers. As mentioned, low molecular weight solvents and ionic liquids are employed as plasticizers. Contrarily, metal oxides are used as fillers. Aziz et al. used Ni metal nanoparticles as fillers [172]. Metal fillers have not been applied to Mg²⁺-ion conductive polymer electrolytes except in this paper. To clarify the effect of metal filler, more research is needed. Sharma et al. added EC-PC and MgAl₂O₄ into PVDF-HFP/Mg(Tf)₂ polymer electrolytes [173]. This system revealed a high transference number of 0.66, which is one of the highest transference numbers in Mg²⁺-ion conductive polymer electrolytes.

The ionic conductivity of filler/plasticizer-containing polymer electrolytes ranges from 10^{-5} to 10^{-3} S cm⁻¹. These values are comparable to other types of polymer electrolytes. Thus, the benefits of using both plasticizers and fillers cannot be emphasized. Currently, the individual effect of plasticizers and fillers on the properties of polymer electrolytes has yet to be fully understood. Thus, the individual effects of plasticizers and fillers must be clarified first. Then, more a complicated system, i.e., polymer electrolytes containing both plasticizers and fillers, should be developed based on the individual effect. Properties of SPEs with plasticizers and fillers are summarized in Table 9.

3. All-Solid-State Mg Battery

3.1. Inorganic Electrolyte

Research on all-solid-state Mg batteries using oxide-based electrolytes is not reported. The Mg²⁺-ion conductivity of the oxide electrolytes is 10^{-6} ~ 10^{-7} S cm⁻¹ at room temperature. This is too low to support ion conduction in all-solid-state batteries operated at room temperature. Thus, an improvement of room temperature ionic conductivity to at least 10^{-4} S cm⁻¹ level is needed first. In the case of MgSc₂Se₄-related materials, although they possess a high Mg²⁺-ionic conductivity, their electronic conductivities are also high. Thus, these materials are not studied for electrolytes for all-solid-state batteries.

All-solid-state Mg batteries using inorganic electrolytes are reported only in borohydride electrolytes, i.e., Mg(BH₄)₂-related materials. The materials are usually prepared by mechanical milling, and all-solid-state cells are constructed by pressing Mg metal anodes

and cathodes onto the solid electrolyte pellets. While these materials demonstrate good Mg stripping/plating behaviors [62,64,65,67,69], only two papers reported that with respect to full cell configurations. In both cases, TiS_2 was used as a cathode, and electrochemical tests were carried out above room temperature (55 and 75 °C) to obtain reasonable capacity. The obtained discharge capacity was about 100 mAh/g, although the C rate was low (141 mAh/g at 0.05 C at 75 °C). Also, capacity decay occurs rapidly (31% capacity retention at the 25th cycle). TiS_2 cathode exhibits large (>100 mAh/g) and stable (>100 cycles) capacities at room temperature and a reasonable C rate (1~2 C) in liquid electrolytes [131]. Thus, the low performance of an all-solid-state battery would be caused by a low conductivity of solid electrolytes and a high impedance/low stability of the cathode/electrolyte interface. Indeed, the interface impedance increased with the cycle number [72].

As mentioned, an improvement of room temperature ionic conductivity is needed to realize all-solid-state Mg batteries using inorganic electrolytes. Additionally, various cathode materials and properties of the electrode/electrolyte interface must be tested and characterized, respectively. In summary, all-solid-state Mg batteries using inorganic electrolytes are still far from realization.

3.2. MOF

In the all-solid-state Mg batteries using MOF-based electrolytes, since MOFs are used to support liquid electrolytes, they can be said “Quasi-solid electrolytes”. Although stable Mg stripping/plating is observed, only one paper reported it in the full cell configuration. The full cell using PTCDA (Perylenetetracarboxilic dianhydride) cathode demonstrates a small discharge capacity of 36 mAh/g at 1 mAh/g at 60 °C. The capacity fade was also large; only 61% of capacity remained in the 3rd cycle. The PTCDA cathode is employed for Na and K batteries [179,180] and reveals a good performance. However, it has not been applied for Mg batteries, even including liquid electrolytes. Therefore, the poor performance of all-solid-state Mg batteries using MOF-based quasi-solid electrolyte has been attributed to some factors, such as the cathode itself, the cathode/electrolyte interface, the electrolyte itself and so on. The usage of common cathode materials like MoS_6 can reduce the factors, facilitating the evaluation of all-solid-state Mg batteries. Consequently, the common cathode materials should be used for the MOF-based quasi-solid electrolytes at this moment.

Since stable Mg stripping/plating was achieved at room temperature in MOF-based solid electrolytes, they would be attractive for all-solid-state Mg battery applications; therefore, studies on cathode side must be carried out intensively.

3.3. Organic Electrolyte

Although studies on SPEs (without fillers and plasticizers) are reported by many groups, SPEs are not applied for all-solid-state Mg batteries. Some groups studied primary Mg batteries using SPEs [90,94,101,103,104,108,115,117,119,123]. Since this review article focuses on rechargeable all-solid-state Mg batteries, the studies on primary batteries are not introduced here. The main reason for the lack of research on SPEs for rechargeable all-solid-state Mg batteries is their relatively low ionic conductivity. The conductivity of most SPEs ranges $10^{-5}\text{--}10^{-7}$ S cm $^{-1}$ at RT. An improvement of the conductivity to $10^{-3}\text{--}10^{-4}$ S cm $^{-1}$ is needed to achieve reasonable performance of all-solid-state Mg batteries. Potato starch [89] and gellan gum [92]-based SPEs exhibit an extremely high ionic conductivity of $\sim 10^{-2}$ S cm $^{-1}$. These are two orders of magnitude higher than other SPEs. A close investigation on these SPEs, such as reproducibility and characterization procedures, should be performed since such a very high conductivity of these SPEs cannot be easily accepted.

Gel Polymer Electrolyte

Gel polymer electrolytes (GPEs) composed of post polymers, Mg salts and plasticizers possess a higher conductivity, $10^{-3}\text{--}10^{-4}$ S cm $^{-1}$, than SPEs. Additionally, their

high flexibility makes battery construction easy. Thus, all-solid-state Mg batteries using GPEs are reported the most. The all-solid-state Mg batteries using GPEs can be operated at room temperature [127,133,140,148]; however, in all cases, initial and steady-state capacities are low. Because stable Mg stripping/plating is observed in GPEs, the cathode itself and the cathode/electrolyte interface would be the reason for the low performance. Detail characterization and post-mortem analysis of the interface and cathode should be carried out.

Ge et al. fabricates pouch cell-type all-solid-state Mg batteries for the first time [127]. Only this study reports the performance of a pouch cell-type all-solid-state Mg battery with GPE. The pouch cell can reduce the weight of battery cases, resulting in a high energy density. Additionally, the authors performed safety tests, such as cutting the pouch cell and flammability tests of GPE and pouch cell. The study is meaningful in verifying the possible application of pouch cell configuration for all-solid-state Mg batteries, although an improvement in the performance of the pouch cells is needed.

Sheha et al. studied dual polymer/liquid electrolytes (Figure 9) [135]. The electrolyte is composed of the following two layers: liquid electrolyte and GPE. Both electrolytes are separated by a glass fiber membrane. The liquid electrolyte (APC, all phenyl complex) and GPE are faced on the cathode and anode (Mg metal) sides, respectively. In the all-solid-state battery, poor contact between a porous electrode and a solid electrolyte increases the impedance of the battery and causes low performance. At the moment, an effective solution for the contact issue has yet to be found. Their concept would be helpful in solving the contact issue. Therefore, the dual electrolyte configuration is likely to be applied for first-generation all-solid-state Mg batteries. The authors reported a high initial capacity using the BaTiO₃ cathode (557 mAh/g at 20 mA/g at 55 °C), but the capacity was rapidly decayed within 15 cycles. The reason for a low cyclability is unclear since the cyclability of the BaTiO₃ cathode has not been tested in liquid electrolytes. The dual electrolytes should be studied using common cathode materials at first. For safety, the usage of the flammable liquid electrolytes must be minimized. The influence of the liquid electrolyte on the safety of the batteries, the formation of CEI (cathode-electrolyte interphase) and the properties of the new interface, i.e., the GPE/liquid electrolyte should be studied for successful application of the dual electrolyte system (In fact, the battery is not pure all-solid-state Mg batteries since the batteries contain a small amount of liquid electrolyte).

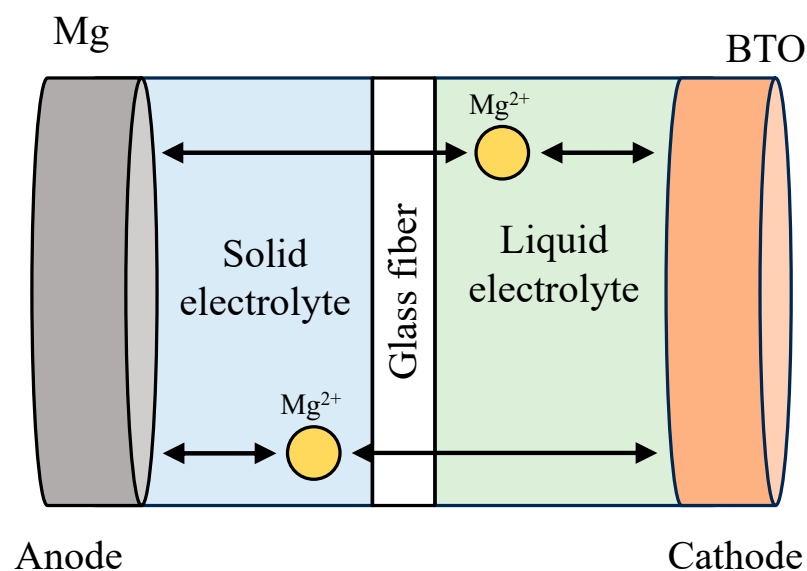


Figure 9. Configuration of Mg battery using the dual GPE/liquid electrolyte (Mg/GPE/APC/BaTiO₃ cathode). Reproduced with permission [135]. Copyright 2020, American Chemical Society.

In the GPE research, Mo₆S₈, which is the most commonly used cathode material, is applied for the all-solid-state battery [127,148]. This facilitates the evaluation of the

all-solid-state batteries since the performance of the cathode has been studied in liquid electrolytes for a long time. Mo_6S_8 cathode provides a high capacity (130 mAh g^{-1} at 0.1 C and 98 mAh g^{-1} at 0.5 C) in liquid electrolytes [181,182]. Contrarily, the all-solid-state batteries using GPEs demonstrate about 70 mAh g^{-1} (68 mAh g^{-1} at 0.1 C [148] and 73 mAh g^{-1} at 0.3 C [127]) even though the same cathode materials are used. Because the ionic conductivity of electrolytes would not largely influence battery performance at such a low C rate, the high impedance at the cathode/electrolyte interface could be a reason for the low performance. Common electrode materials should be used for all-solid-state batteries more intensively. It is interesting to note that better battery performance was obtained in the PECH-OH-based GPE compared to the PTHF-based GPE. As shown in Table 6, the PTHF-based GPE revealed about two orders of magnitude higher Mg^{2+} -ion conductivity than the PECH-OH-based GPE. This is a good example that battery performance is determined by not only the properties of electrolytes. GPE is the most promising for all-solid-state Mg batteries at this moment. The ionic conductivity of GPEs is comparable to Li^+ -ion conductive polymer electrolytes. Thus, compatibility with electrodes and properties of the electrode/electrolyte interface would determine the performance of all-solid-state Mg batteries. Many studies on GPEs are reported, while their application to all-solid-state Mg batteries is not researched intensively. Such study is strongly required, not only simple studies on properties of GPEs, to realize all-solid-state Mg batteries.

3.4. Organic–Inorganic Composite Electrolytes

Only three papers have been reported in terms of all-solid-state Mg batteries using the organic–inorganic composite electrolytes recently [168,177,178]. Compared with GPEs, all-solid-state Mg batteries with composite electrolytes demonstrate a better initial performance and cyclability. Particularly, when SPEs contain both fillers and plasticizers, a very stable cyclability was achieved, although only two papers were reported. Both papers exhibited 99% capacity retention at the 100th cycle [177] and 98% capacity retention at the 70th cycle [178]. The compatibility of polymer electrolytes with electrodes, especially cathodes, is likely to be improved by adding fillers. Wang et al. successfully prepared the pouch cell-type all-solid-state Mg batteries [178]. The cell demonstrated excellent performance. However, the solid electrolyte contained two salts, $\text{Mg}(\text{BH}_4)_2$ and LiBH_4 . The ratio of Mg/Li is $0.1/1.5$. Thus, it is unclear the influence of Li intercalation on observed capacity.

Despite fewer examples, fillers would improve the stability of all-solid-state Mg batteries. The application of the organic–inorganic composite electrolytes for all-solid-state Mg batteries must be studied more intensively. Although pouch cell-type all-solid-state battery was reported, common coin cell configuration and cathode materials should be adopted at this moment because the application of organic–inorganic composite electrolytes for all-solid-state Mg battery is still infant stage. Properties of all-solid-state Mg batteries are summarized in Table 10.

Table 10. Properties of all-solid-state Mg batteries.

Electrolyte	Cathode	Initial Capacity	Capacity Retention	Temp. (°C)	Note	Ref.
Borohydrides						
Mg(BH ₄)(NH ₂)	Pt	-	-	-	Mg plating on Pt	[62]
Mg(BH ₄)(NH ₃ BH ₃) ₂	Mo	-	-	-	Mg plating on Mo	[65]
0.4Mg(BH ₄) ₂ •NH ₃ - 0.6Mg(BH ₄) ₂ •2NH ₃ @MgO	Mg	-	-	60	Stable Mg stripping/plating more than 100 cycles at 0.25 mA cm ⁻²	[69]
Mg(en) ₁ (BH ₄) ₂	Pt	-	-	60	Stable Mg stripping/plating in 20 cycles at 10 mV s ⁻¹	[64]
Mg(BH ₄) ₂ 1.5NH ₃ -YSZ	Mg	-	-	60	Stable Mg stripping/plating in 300 cycles at 0.1 mA cm ⁻²	[67]
Mg(BH ₄) ₂ •2NH ₃	TiS ₂	141 mAh/g at 0.05C	31% at 25th cycle	75	111 mAh/g at 0.2C, 72 mAh/g at 0.5C	[72]
Mg(BH ₄) ₂ •1.5THF-MgO	TiS ₂	94 mAh/g at C/50	32% at 5th cycle	55	SS current collector was oxidized	[70]
MOF						
Mg(TFSI) ₂ /MgCl ₂ /DME in MOF-74	Mg	-	-	RT	Stable Mg stripping/plating in 100 cycles at 0.05 mA cm ⁻²	[78]
Mgbp3dc in α -Mg ₃ (HCOO) ₆ /DMF	Mg	-	-	RT	Stable Mg stripping/plating in 8 cycles at 0.1 μ A cm ⁻²	[75]
Mg(TFSI) ₂ /[EMIM][TFSI] in UiO-66	PTCDA	36 mAh/g at 1 mA/g	61% at 3rd cycle	60	Stable Mg stripping/plating more than 200 cycles at 3.14 μ A cm ⁻²	[76]
GPE						
PVDF-TEGDME-Mg(Tf) ₂	BaTiO ₃	557 mAh/g at 20 mA/g	12% at 15th cycle	55	<ul style="list-style-type: none"> Full cell configuration: Mg/SE/APC/Cathode Stable Mg stripping/plating more than 25 cycles at 0.02 mA cm⁻² 	[135]
PECH-OH-MgCl ₂ -TEGDME	Mo ₆ S ₈	73 mAh/g at 0.3 C	84% at 100th cycle	30	Pouch cell data	[127]
PVDF-HFP-Mg(Tf) ₂ -SN + EMITf	MnO ₂	40 mAh/g at 38 μ A cm ⁻²	12.5% at 8th cycle	RT		[140]
PTHF-MgBOR	Mo ₆ S ₈	68 mAh/g at 0.1 C	74% at 100th cycle	25	Stable Mg stripping/plating more than 1000 cycles at 0.1 mA cm ⁻²	[148]

Table 10. *Cont.*

Electrolyte	Cathode	Initial Capacity	Capacity Retention	Temp. (°C)	Note	Ref.
PVDF/HFP-MgCl ₂ /AlCl ₃ -TEGDME	MoS ₂	121 mAh/g at 40 mA/g	58% at 1700th cycle	25	Stable Mg stripping/plating more than 400 cycles at 1.0 mA cm ⁻²	[133]
			Filler			
PVDF-HFP/PVAc-Mg(ClO ₄) ₂ -MgTiO ₃	Mo ₆ S ₈	120 mAh/g at 0.5 C	87% at 30th cycle	RT		[168]
			SPE + filler + plasticizer			
PVDF-HFP-Mg(TFSI) ₂ -SiO ₂	TiO ₂	129 mAh/g at 50 mA/g	99% at 100th cycle	RT	Stable Mg stripping/plating more than 100 cycles at 0.2 mA cm ⁻²	[177]
PTHF- Mg(BH ₄) ₂ /LiBH ₄ -Diglyme-TiO ₂	TiS ₂	225 mAh/g at 0.5 C	98% at 70th cycle	22	Stable Mg stripping/plating more than 100 cycles at 0.1 mA cm ⁻²	[178]

4. Challenges

The all-solid-state Mg battery is a good option to replace LIBs due to high safety, energy density and resource abundance. Thanks to the many efforts of researchers, technologies for the all-solid-state Mg battery have progressed significantly. Despite the significant progress, further research is still required to realize the all-solid-state Mg battery. Herein, the challenges are summarized.

(1) Inorganic electrolytes

The Mg^{2+} -ion conductivity of current ceramic electrolytes is $10^{-6}\sim10^{-7} \text{ S cm}^{-1}$ at room temperature (except [33,35,59]). Even with hydride-based inorganic electrolytes, the conductivity is $\sim10^{-5} \text{ S cm}^{-1}$. For all-solid-state Mg batteries, the required conductivity is $>\sim10^{-4} \text{ S cm}^{-1}$ at room temperature to ensure room temperature operation. Thus, an improvement in ionic conductivity must be investigated in inorganic electrolytes. Some groups have studied the Mg^{2+} -ion conductivity of ceramic electrolytes intensively; however, an effective solution to enhance the conductivity is yet to be found at this moment. Thus, thin film ceramic electrolytes would effectively compensate for the low conductivity. Currently, only one paper is reported with respect to thin film ceramic electrolytes [58]. The thin film ceramic electrolytes should be studied more intensively. Adding inorganic fillers will likely improve the ionic conductivity in the hydride-based electrolytes [67,68]. The effect of fillers should be a good research topic for further study.

(2) Study on Mg salts

Compared to inorganic electrolytes, organic polymer electrolytes are more promising in the application of all-solid-state Mg batteries at this moment. Various polymer hosts have been studied. On the other hand, a systematic study on Mg salts is not carried out. Fichtner et al. reported the corrosion of the battery case and current collectors by Cl-contained salt [148]. Although various types of Mg salts, such as $MgSO_4$, $MgCl_2$, $Mg(ClO_4)_2$, $Mg(TFSI)_2$, $Mg(NO_3)_2$ and $Mg(Tf)_2$, have been employed so far, a suitable Mg salt for the all-solid-state Mg battery is still under investigation. Therefore, the effect of Mg salts on the properties of SPEs (and GPEs) and the performances of all-solid-state Mg batteries should be studied systematically.

(3) Mechanical properties of solid electrolytes

High flexibility is one of the benefits of SPEs and GPEs, which facilitates the construction of the all-solid-state Mg battery. However, quantitative evaluation of the flexibility, i.e., mechanical properties, has not been carried out yet. The mechanical properties of solid electrolytes influence cell pressure, contact with electrodes, suppression of Mg dendrite formation, etc., significantly. Consequently, both the electrochemical and mechanical properties of SPEs and GPEs must be characterized precisely.

(4) Construction of all-solid-state Mg battery

As mentioned in a previous section, most research focuses on solid electrolytes and only some papers try to fabricate all-solid-state Mg batteries. The compatibility of solid electrolytes with an all-solid-state Mg battery cannot be evaluated by only ionic conductivity, electrochemical window, transference number, etc. Therefore, solid electrolytes must be evaluated in all-solid-state batteries in addition to the above-mentioned properties. Particularly, the properties of the electrode/solid electrolyte interface that largely affect the performance of all-solid-state Mg batteries can be characterized only in the all-solid-state battery configuration.

(5) Energy density

At the moment, the energy density of an all-solid-state Mg battery cannot be discussed since the development is still in the infant stage. To improve the energy density, one good strategy is a decrease in electrolyte thickness. A thin electrolyte can reduce the volume

and weight of the all-solid-state battery, resulting in an enhancement of the energy density. Therefore, the decrease in the thickness of electrolytes must be studied.

(6) Cathode materials

Some groups employ novel cathode materials for the all-solid-state Mg batteries. In this case, the performance of the cathode material is unknown. Thus, it is impossible to clarify the reason for the poor performance of the all-solid-state Mg battery, i.e., the cathode itself or other components. Common cathode materials such as Mo_6S_8 and TiS_2 , which are well characterized in liquid electrolytes, should be used to characterize and evaluate the all-solid-state Mg batteries. After that, the development of cathode materials for all-solid-state batteries would be carried out.

An all-solid-state Mg battery would replace current LIBs owing to high safety, energy density and resource abundance, although the research is still infant stage. To realize the all-solid-state Mg battery, above mentioned studies must be carried out intensively. Additionally, research on an Mg battery using liquid electrolytes should be referred to, especially for the cathode selection. The following possible strategy is suggested: (1) Development of polymer-based solid electrolytes (with/without plasticizers and fillers), (2) Investigation of compatibility with cathode materials in all-solid-state batteries (common cathodes will be used at first, then novel cathodes for all-solid-state batteries will be studied), (3) Decreasing thickness of electrolytes and applying a pouch cell configuration to improve energy density. The first-generation all-solid-state Mg battery would employ polymer-based solid electrolytes because it would need more time to develop inorganic electrolytes. Most probably, dual polymer/liquid electrolytes, as shown in Figure 9, would be employed to solve poor contact between porous cathodes and solid electrolytes. Then, full all-solid-state Mg batteries could be developed based on knowledge and experiences obtained in dual polymer/liquid electrolytes. Ceramic electrolytes could be applied after the realization of SPE and GPE-based all-solid-state Mg batteries.

Author Contributions: J.P. and G.J.; analysis, writing—original draft preparation, K.Z.W. and M.K.; writing—review and editing, M.K.; supervision. All authors have read and agreed to the published version of the manuscript.

Funding: This research received no external funding.

Conflicts of Interest: The authors declare no conflict of interest.

References

- Winter, M.; Barnett, N.; Xu, K. Before Li ion batteries. *Chem. Rev.* **2018**, *118*, 11433–11456. [[CrossRef](#)] [[PubMed](#)]
- Li, M.; Lu, J.; Chen, Z.W.; Amine, K. 30 years of lithium-ion batteries. *Adv. Mater.* **2018**, *30*, 1800561. [[CrossRef](#)] [[PubMed](#)]
- Li, Q.; Chen, D.; Tan, H.; Zhang, X.; Rui, X.; Yu, Y. 3D porous V_2O_5 architectures for high-rate lithium storage. *J. Energy Chem.* **2020**, *40*, 15–21. [[CrossRef](#)]
- Zeng, J.; Peng, C.; Wang, R.; Cao, C.; Wang, X.; Liu, J. Micro-sized $\text{FeS}_2@\text{FeSO}_4$ core-shell composite for advanced lithium storage. *J. Alloys Compd.* **2020**, *814*, 151922. [[CrossRef](#)]
- Armand, M.; Tarascon, J.M. Building better batteries. *Nature* **2008**, *451*, 652–657. [[CrossRef](#)]
- Whittingham, M.S. Ultimate limits to intercalation reactions for lithium batteries. *Chem. Rev.* **2014**, *114*, 11414–11443. [[CrossRef](#)]
- Xu, W.; Wnag, J.L.; Ding, F.; Chen, X.L.; Nasybutin, E.; Zhang, Y.H.; Zhang, J.G. Lithium metal anodes for rechargeable batteries. *Energy Environ. Sci.* **2014**, *7*, 513–537. [[CrossRef](#)]
- Wang, Y.; Liang, J.; Song, X.; Jin, Z. Recent progress in constructing halogenated interfaces for highly stable lithium metal anodes. *Energy Storage Mater.* **2023**, *54*, 732–775. [[CrossRef](#)]
- Sarkar, S.; Thangadurai, V. Critical current densities for high-performance all-solid-state Li-metal batteries: Fundamentals mechanisms, interfaces materials and applications. *ACS Energy Lett.* **2022**, *7*, 1492–1527. [[CrossRef](#)]
- Feng, Z.; Kotobuki, M.; Song, S.; Lai, M.O.; Lu, L. Review on solid electrolytes for all-solid-state lithium-ion batteries. *J. Power Sources* **2018**, *389*, 198–213. [[CrossRef](#)]
- Hebie, S.; Mgo, H.P.K.; Lepretre, J.-C.; Iojoiu, C.; Cointeaux, L.; Berthelot, R.; Alloin, F. Electrolyte based on easily synthesized, low cost triphenolate-borohydride salt for high performance $\text{Mg}(\text{TFSI})_2$ -glyme rechargeable magnesium batteries. *ACS Appl. Mater. Interfaces* **2017**, *9*, 28377–28385. [[CrossRef](#)]
- Wei, C.; Tan, L.; Zhang, Y.; Xi, B.; Xiong, S.; Feng, J.; Qian, Y. Highly reversible Mg metal anodes enabled by interfacial liquid metal engineering for high-energy Mg-S batteries. *Energy Storage Mater.* **2022**, *48*, 447–457. [[CrossRef](#)]

13. Jackle, M.; Helmbrecht, K.; Smits, M.; Stottmeister, D.; Gross, A. Self-diffusion barriers: Possible descriptors for dendrite growth in batteries. *Energy Environ. Sci.* **2018**, *11*, 3400–3407. [[CrossRef](#)]
14. Kotobuki, M. Recent progress of ceramic electrolytes for post Li and Na batteries. *Funct. Mater. Lett.* **2021**, *14*, 2130003. [[CrossRef](#)]
15. Shuai, H.; Xu, J.; Huang, K. Progress in retrospect of electrolytes for secondary magnesium batteries. *Coord. Chem. Rev.* **2020**, *422*, 213478. [[CrossRef](#)]
16. Chen, C.; Wang, K.; He, H.; Hanc, E.; Kotobuki, M.; Lu, L. Processing and properties of garnet-type $\text{Li}_7\text{La}_3\text{Zr}_2\text{O}_{12}$ ceramic electrolytes. *Small* **2022**, *19*, 2205550. [[CrossRef](#)] [[PubMed](#)]
17. Wang, C.; Fu, K.; Kammampata, S.P.; McOwen, D.W.; Samson, A.J.; Zhang, L.; Hits, G.T.; Nolan, A.M.; Wachman, E.D.; Mo, Y.; et al. Garnet-type solid-state electrolytes: Materials, interfaces and batteries. *Chem. Rev.* **2020**, *120*, 4257–4300. [[CrossRef](#)] [[PubMed](#)]
18. Miao, G.; CHongyang, Y.; Tengfei, Z.; Xuebin, Y. Solid state electrolytes for rechargeable magnesium-ion batteries: From structure to mechanism. *Small* **2022**, *18*, 2106981.
19. Stefania, F.; Marisa, F.; Belen, B.G.A.; Matteo, B.; Segio, B.; Michele, P.; Claudio, G. Solid-state post Li metal ion batteries: A sustainable forthcoming reality? *Adv. Energy Mater.* **2021**, *11*, 2100785.
20. Yabuuchi, N.; Kubota, K.; Dahbi, M.; Komaba, S. Research development on Sodium-ion batteries. *Chem. Rev.* **2014**, *114*, 11636–11682. [[CrossRef](#)]
21. Yan, B.; Wang, Z.; Ren, H.; Lu, X.; Qu, Y.; Liu, W.; Jiang, K.; Kotobuki, M. Interfacial modification of $\text{Na}_3\text{Zr}_2\text{Si}_2\text{PO}_{12}$ solid electrolyte by femtosecond laser etching. *Ionics* **2023**, *29*, 865–870. [[CrossRef](#)]
22. Nakayama, M.; Nakano, K.; Harada, M.; Tanibata, N.; Takeda, H.; Noda, Y.; Kobatashi, R.; Karasuyama, M.; Takeuchi, I.; Kotobuki, M. Na superionic conductor-type $\text{LiZr}_2(\text{PO}_4)_3$ as a promising solid electrolyte for use in all-solid-state Li metal batteries. *Chem. Comm.* **2022**, *58*, 9328. [[CrossRef](#)] [[PubMed](#)]
23. Kotobuki, M.; Yanagiya, S. Li-ion conductivity of NASICON-type $\text{Li}_{1+2x}\text{Zr}_{2-x}\text{Ca}_x(\text{PO}_4)_3$ solid electrolyte prepared by spark plasma sintering. *J. Alloys Compd.* **2021**, *862*, 158641. [[CrossRef](#)]
24. Kotobuki, M.; Koishi, M. Preparation of $\text{Li}_{1.3}\text{Al}_{0.3}\text{Ti}_{1.7}(\text{PO}_4)_3$ solid electrolyte via a sol-gel method using various Ti Sources. *J. Asian Ceram. Soc.* **2020**, *8*, 891–897. [[CrossRef](#)]
25. Kotobuki, M.; Koishi, M. Preparation of $\text{Li}_{1.5}\text{Al}_{0.5}\text{Ti}_{1.5}(\text{PO}_4)_3$ solid electrolyte via a sol-gel route using various Al sources. *Ceram. Int.* **2013**, *39*, 4645–4649. [[CrossRef](#)]
26. Hayamizu, K.; Haishi, T. Ceramic-glass pellet thickness and Li diffusion in NASICON-type LAGP ($\text{Li}_{1.5}\text{Al}_{0.5}\text{Ge}_{1.5}(\text{PO}_4)_3$) studied by pulsed field gradient NMR spectroscopy. *Solid State Ion.* **2022**, *380*, 115924. [[CrossRef](#)]
27. Yan, B.; QU, Y.; Ren, H.; Lu, X.; Wang, Z.; Liu, W.; Wang, Y.; Kotobuki, M.; Jiang, K. A solid-liquid composite electrolyte with a vertical microporous $\text{Li}_{1.5}\text{Al}_{0.5}\text{Ge}_{1.5}(\text{PO}_4)_3$ skeleton that prepared by femtosecond laser structuring and filled with ionic liquid. *Mater. Chem. Phys.* **2022**, *287*, 126265. [[CrossRef](#)]
28. Lee, W.; Tamura, S.; Imanaka, N. Synthesis and characterization of divalent ion conductors with NASICON-type structures. *J. Asian Ceram. Soc.* **2019**, *7*, 221–227. [[CrossRef](#)]
29. Shao, Y.J.; Zhong, G.M.; Lu, Y.X.; Liu, L.L.; Zhao, C.L.; Zhang, Q.Q. A novel NASICON-based glass-ceramic composite electrolyte with enhanced Na-ion conductivity. *Energy Storage Mater.* **2019**, *23*, 514–521. [[CrossRef](#)]
30. Ikeda, S.; Takahashi, M.; Ishikawa, J.; Ito, K. Solid electrolytes with multivalent cation conduction. 1. Conducting species in MgZrPO_4 system. *Solid State Ion.* **1987**, *23*, 125–129. [[CrossRef](#)]
31. Nakano, K.; Noda, Y.; Tanibata, N.; Nakayama, M.; Kajihara, K.; Kanamura, K. Computational investigation of the Mg-ion conductivity and phase stability of $\text{MgZr}_4(\text{PO}_4)_6$. *RSC Adv.* **2019**, *9*, 12590–12595. [[CrossRef](#)] [[PubMed](#)]
32. Kawamura, J.; Morota, K.; Kuwata, N.; Nakamura, Y.; Maekawa, H.; Hattori, T.; Imanaka, N.; Okazaki, Y.; Adachi, G.-Y. High temperature ^{31}P NMR study on Mg^{2+} ion conductors. *Solid State Comm.* **2001**, *120*, 295–298. [[CrossRef](#)]
33. Anuar, N.K.; Adnan, S.B.R.S.; Jaafar, M.H.; Mohamed, N.S. Studies on structural and electrical properties of $\text{Mg}_{0.5+y}(\text{Zr}_{2-y}\text{Fe}_y)_2(\text{PO}_4)_3$ ceramic electrolytes. *Ionics* **2016**, *22*, 1125–1133. [[CrossRef](#)]
34. Tamura, S.; Yamane, M.; Hoshino, Y.; Imanaka, N. Highly conducting divalent Mg^{2+} cation solid electrolytes with well-ordered three-dimensional network structure. *J. Solid State Chem.* **2016**, *235*, 7–11. [[CrossRef](#)]
35. Anuar, N.K.; Mohamed, N.S. Structural and electrical properties of novel $\text{Mg}_{0.9+0.5y}\text{Zn}_{0.4}\text{Al}_y\text{Zr}_{1.6-y}(\text{PO}_4)_3$ ceramic electrolytes synthesized via nitrate sol-gel method. *J. Sol-Gel Sci. Technol.* **2016**, *80*, 249–258. [[CrossRef](#)]
36. Halim, Z.A.; Adnan, S.B.R.S.; Mohamed, N.S. Effect of sintering temperature on the structural, electrical and electrochemical properties of novel $\text{Mg}_{0.5}\text{Si}_2(\text{PO}_4)_3$ ceramic electrolytes. *Ceram. Int.* **2016**, *42*, 4452–4461. [[CrossRef](#)]
37. Su, J.; Tsuruoka, T.; Tsujita, T.; Nishitani, Y.; Nakura, K.; Terabe, K. Aromatic layer deposition of a magnesium phosphate solid electrolyte. *Chem. Mater.* **2019**, *31*, 5566–5575. [[CrossRef](#)]
38. Takeda, H.; Nakano, K.; Tanibata, N.; Nakayama, M. Novel Mg-ion conductive oxide of μ -cordierite $\text{Mg}_{0.6}\text{Al}_{1.2}\text{Si}_{1.8}\text{O}_6$. *Sci. Technol. Adv. Mater.* **2020**, *21*, 131–138. [[CrossRef](#)]
39. Omote, A.; Yotsuhashi, S.; Zenitani, Y.; Yamada, Y. High ion conductivity in $\text{MgHf}(\text{WO}_4)_3$ solids with ordered structure: 1-D alignments of Mg^{2+} and Hf^{4+} ions. *J. Am. Ceram. Soc.* **2011**, *94*, 2285–2288. [[CrossRef](#)]
40. Fujii, Y.; Kobayashi, M.; Miura, A.; Rosero-Navarro, N.C.; Li, M.; Sun, J.; Kotobuki, M.; Tadanaga, K. Fe-P-S electrodes for all-solid-state lithium secondary batteries using sulfide-based solid electrolytes. *J. Power Sources* **2020**, *449*, 227576. [[CrossRef](#)]

41. Yamanaka, T.; Hayashi, A.; Yamauchi, A.; Tatsumisago, M. Preparation of magnesium ion conducting $MgS-P_2S_5-MgI_2$ glasses by a mechanochemical technique. *Solid State Ion.* **2014**, *262*, 601–603. [CrossRef]
42. Canepa, P.; Bo, S.-H.; Gautam, G.S.; Key, B.; Richards, W.D.; Shi, T.; Tian, Y.; Wang, Y.; Li, J.; Ceder, G. High magnesium mobility in ternary spinel chalcogenides. *Nat. Comm.* **2017**, *8*, 1759. [CrossRef] [PubMed]
43. Koishi, M.; Kotobuki, M. Preparation of Y-doped $Li_7La_3Zr_2O_{12}$ by co-precipitation method. *Ionics* **2022**, *28*, 2065–2072. [CrossRef]
44. Wang, L.-P.; Zhao-Karger, Z.; Klein, F.; Chable, J.; Braun, T.; Schuer, A.R.; Wang, C.-R.; Guo, Y.-G.; Fichtner, M. $MgSc_2Se_4$ -magnesium solid ionic conductor for all-solid-state Mg batteries? *ChemSusChem* **2019**, *12*, 2286–2293. [CrossRef] [PubMed]
45. Kundu, S.; Solomatin, N.; Kauffmann, Y.; Kraytsberg, A.; Ein-Eli, Y. Revealing and excluding the root cause of the electronic conductivity in Mg-ion $MgSc_2Se_4$ solid electrolyte. *Appl. Mater. Today* **2021**, *23*, 100998. [CrossRef]
46. Kundu, S.; Solomatin, N.; Kraytsberg, A.; Ein-Eli, Y. $MgSc_2Se_4$ solid electrolyte for rechargeable Mg batteries: An electric field-assisted all-solid-state synthesis. *Energy Technol.* **2022**, *10*, 2200896. [CrossRef]
47. Clemenceau, T.; Andriamady, N.; Kumar, M.K.; Bardran, A.; Avila, V.; Dhal, K.; Hopkins, M.; Vendrell, X.; Marshall, D.; Raj, R. Flash sintering of Li-ion conducting ceramic in a few seconds at 850 °C. *Scr. Mater.* **2019**, *172*, 1–5. [CrossRef]
48. Yan, B.; Kang, L.; Kotobuki, M.; He, L.; Liu, B.; Jiang, K. Boron group element doping of $Li_{1.5}Al_{0.5}Ge_{1.5}(PO_4)_3$ based on microwave sintering. *J. Solid State Electrochem.* **2021**, *25*, 527–534. [CrossRef]
49. Wang, C.; Ping, W.; Bai, Q.; Cui, H.; Hensleigh, R.; Wang, R.; Brozena, A.H.; Xu, Z.; Dai, J.; Pei, Y.; et al. A general method to synthesize and sinter bulk ceramics in seconds. *Science* **2020**, *368*, 521–526. [CrossRef]
50. Anuar, N.K.; Adnan, S.B.R.S.; Mohamed, N.S. Characterization of $Mg_{0.5}Zr_2(PO_4)_3$ for potential use as electrolyte in solid state magnesium batteries. *Ceram. Int.* **2014**, *40*, 13719–13727. [CrossRef]
51. Mohammed, A.; Kale, G.M. Novel sol-gel synthesis of $MgZr_4P_6O_{24}$ composite solid electrolyte and newer insight into the Mg^{2+} -ion conducting properties using impedance spectroscopy. *J. Phys. Chem. C* **2016**, *120*, 17909–17915.
52. Imanaka, N.; Okazaki, Y.; Adachi, G.-Y. Divalent magnesium ion conducting characteristics in phosphate based solid electrolyte composites. *J. Mater. Chem. C* **2000**, *10*, 1431–1435. [CrossRef]
53. Imanaka, N.; Okazaki, Y.; Adachi, G. Optimization of divalent magnesium ion conduction in phosphate based polycrystalline solid electrolytes. *Ionics* **2001**, *7*, 440–446. [CrossRef]
54. Liang, B.; Kreshishian, V.; Liu, S.; Yi, E.; Jia, D.; Zhou, Y.; Kieffer, J.; Ye, B.; Kaine, R.M. Processing liquid-feed flame spray pyrolysis synthesized $Mg_{0.5}Ce_{0.2}Zr_{1.8}(PO_4)_3$ nanopowders to free standing thin films and pellets as potential electrolytes in all-solid-state Mg batteries. *Electrochim. Acta* **2018**, *272*, 144–153. [CrossRef]
55. Kajihara, K.; Nagano, H.; Tsujita, T.; Munakata, H.; Kanamura, K. High-temperature conductivity measurements of magnesium-ion-conducting solid oxide $Mg_{0.5-x}(Zr_{1-x}Nb_x)_2(PO_4)_3$ ($x = 0.15$) using Mg metal electrodes. *J. Electrochem. Soc.* **2017**, *164*, A2183–A2185. [CrossRef]
56. Mustafa, M.; Rani, M.S.A.; Adnan, S.B.R.S.; Salleh, F.M.; Mohamed, N.S. Characteristics of new $Mg_{0.5}(Zr_{1-x}Sn_x)_2(PO_4)_3$ NASICON structured compound as solid electrolytes. *Ceram. Int.* **2020**, *46*, 28145–28155. [CrossRef]
57. Imanaka, N.; Okazaki, Y.; Adachi, G. Divalent magnesium ionic conduction in $Mg_{1-2x}(Zr_{1-x}Nb_x)_4P_6O_{24}$ ($x = 0\text{--}0.4$) solid solutions. *Electrochim. Solid State Lett.* **2000**, *3*, 327–329. [CrossRef]
58. Liu, S.; Zhou, C.; Wang, Y.; Yi, E.; Wang, W.; Kieffer, J.; Laine, R.M. Processing combustion synthesized $Mg_{0.5}Zr_2(PO_4)_3$ nanopowders to thin films as potential solid electrolytes. *Electrochim. Comm.* **2020**, *116*, 106753. [CrossRef]
59. Halim, Z.A.; Adnan, S.B.R.S.; Salleh, F.M.; Mohamed, N.S. Effects of Mg^{2+} interstitial ion on the properties of $Mg_{0.5+x/2}Si_{2-x}Al_x(PO_4)_3$ ceramic electrolytes. *J. Magnes. Alloy* **2017**, *5*, 439–447. [CrossRef]
60. Sulaiman, M.; Su, N.C.; Mohamed, N.S. Sol-gel synthesis and characterization of β - $MgSO_4$: $Mg(NO_3)_2$ -MgO composite solid electrolyte. *Ionics* **2017**, *23*, 443–452. [CrossRef]
61. Matsuo, M.; Oguchi, H.; Sato, T.; Takamura, H.; Tsuchida, E.; Ikeshoji, T.; Orimo, S.-I. Sodium and magnesium ionic conduction in complex hydrides. *J. Alloys Compd.* **2013**, *580*, S98–S101. [CrossRef]
62. Higashi, S.; Miwa, K.; Aoki, M.; Takechi, K. A novel inorganic solid state ion conductor for rechargeable Mg batteries. *Chem. Comm.* **2014**, *50*, 1320. [CrossRef] [PubMed]
63. Ruyet, R.L.; Berthelot, R.; Salager, E.; Florian, P.; Fleutot, B.; Janot, R. Investigation of $Mg(BH_4)(NH_2)$ -based composite materials with enhanced Mg^{2+} ionic conductivity. *J. Phys. Chem. C* **2019**, *123*, 10756–10763. [CrossRef]
64. Roedern, E.; Kuhnel, R.-S.; Remhof, A.; Battaglia, C. Magnesium ethylenediamine borohydride as solid-state electrolyte for magnesium batteries. *Sci. Rep.* **2017**, *7*, 46189. [CrossRef] [PubMed]
65. Kis, K.; Kim, S.; Inukai, M.; Oguchi, H.; Takagi, S.; Orimo, S.-I. Magnesium borohydride ammonia borane as a magnesium ionic conductor. *ACS Appl. Energy Mater.* **2020**, *3*, 3174–3179. [CrossRef]
66. Luo, X.; Rawal, A.; Cazorla, C.; Aguey-Zinsou, K.F. Facile self-forming superionic conductors based on complex borohydride surface oxidation. *Adv. Sus. Syst.* **2020**, *4*, 1900113. [CrossRef]
67. Wang, Q.; Li, H.; Zhang, R.; Liu, Z.; Deng, H.; Cen, W.; Yan, Y.; Chen, Y. Oxygen vacancies boosted fast Mg^{2+} migration in solids at room temperature. *Energy Storage Mater.* **2022**, *51*, 630–637. [CrossRef]
68. Yan, Y.; Grinderslev, J.B.; Burankova, T.; Wei, S.; Embs, J.P.; Skibsted, J.; Jensen, T.R. Fast room-temperature Mg^{2+} conductivity in $Mg(BH_4)_2 \cdot 1.6NH_3 \cdot Al_2O_3$ nanocomposites. *J. Phys. Chem. Lett.* **2022**, *13*, 2211–2216. [CrossRef]
69. Yan, Y.; Grinderslev, J.B.; Jorgensen, M.; Skov, L.N.; Skibsted, J.; Jensen, T.R. Ammine magnesium borohydride nanocomposites for all-solid-state magnesium batteries. *ACS Appl. Energy Mater.* **2020**, *3*, 9264–9270. [CrossRef]

70. Skov, L.N.; Grinderslev, J.B.; Rosenkranz, A.; Lee, Y.-S.; Jensen, T.R. Towards solid-state magnesium batteries: Ligand-assisted superionic conductivity. *Batter. Supercaps* **2022**, *5*, e202200163. [[CrossRef](#)]
71. Ruyet, R.L.; Fleutot, B.; Berthelot, R.; Benabed, Y.; Hatier, G.; Filinchuk, Y.; Janot, R. Mg₃(BH₄)₄(NH₂)₂ as inorganic solid electrolyte with high Mg²⁺ ionic conductivity. *ACS Appl. Energy Mater.* **2020**, *3*, 6093–6097. [[CrossRef](#)]
72. Pang, Y.; Nie, Z.; Xu, F.; Sun, L.; Yang, J.; Sun, D.; Fang, F.; Zheng, S. Borohydride ammonium solid electrolyte design for all-solid-state Mg batteries. *Energy Environ. Mater.* **2022**, *e12527*. [[CrossRef](#)]
73. Rouhani, F.; Rafizadeh-Masuleh, F.; Morsali, A. Highly electroconductive metal-organic framework: Tunable by metal ion sorption quantity. *J. Am. Chem. Soc.* **2019**, *141*, 11173–11182. [[CrossRef](#)]
74. Yanai, N.; Uemura, T.; Horike, S.; Shimomura, S.; Kiragawa, S. Inclusion and dynamics of a polymer-Li salt complex in coordination nanochannels. *Chem. Comm.* **2011**, *47*, 1722–1724. [[CrossRef](#)] [[PubMed](#)]
75. Hassan, H.K.; Farkas, A.; Varzi, A.; Jacob, T. Mixed metal-organic frameworks as efficient semi-solid electrolytes for magnesium-ion batteries. *Batter. Supercaps* **2022**, *5*, e202200260. [[CrossRef](#)]
76. Wei, Z.; Maile, R.; Rieger, L.M.; Rohnke, M.; Muller-Buschbaum, K.; Janek, J. Ionic liquid-incorporated metal-organic framework with high magnesium ion conductivity for quasi-solid-state magnesium batteries. *Batter. Supercaps* **2022**, *5*, e202200318. [[CrossRef](#)]
77. Zheng, Y.; Guo, J.; Ning, D.; Hunag, Y.; Lei, W.; Li, J.; Li, J.; Schuck, G.; Shen, J.; Guo, Y.; et al. Design of metal-organic frameworks for improving pseudo-solid-state magnesium-ion electrolytes: Open metal sites, isoreticular expansion and framework topology. *J. Mater. Sci. Technol.* **2023**, *144*, 15–27. [[CrossRef](#)]
78. Luo, J.; Li, Y.; Zhang, H.; Wang, A.; Lo, W.-S.; Dong, Q.; Wong, N.; Povinelli, C.; Shao, Y.; Chereddy, S.; et al. A metal-organic framework thin film for selective Mg²⁺ transport. *Angew. Chem. Int. Ed.* **2019**, *58*, 15313–15317. [[CrossRef](#)] [[PubMed](#)]
79. Aubrey, M.L.; Ameloot, R.; Wiers, B.M.; Long, J.R. Metal-organic frameworks as solid magnesium electrolytes. *Energy Environ. Sci.* **2014**, *7*, 667–671. [[CrossRef](#)]
80. Park, S.S.; Tukchinsky, Y.; Dinca, M. Single-ion Li⁺, Na⁺ and Mg²⁺ solid electrolytes supported by a mesoporous anionic Cu-azolate metal-organic framework. *J. Am. Chem. Soc.* **2017**, *139*, 13260–13263. [[CrossRef](#)]
81. Miner, E.M.; Park, S.S.; Dinca, M. High Li⁺ and Mg²⁺ conductivity in a Cu-azolate metal-organic framework. *J. Am. Chem. Soc.* **2019**, *141*, 4422–4427. [[CrossRef](#)] [[PubMed](#)]
82. Yoshida, Y.; Yamada, T.; Jing, Y.; Toyao, T.; Shimizu, K.-I.; Sadakiyo, M. Super Mg²⁺ conductivity around 10⁻³ S cm⁻¹ observed in a porous metal-organic framework. *J. Am. Chem. Soc.* **2022**, *144*, 8669–8675.
83. Walke, P.; Venturini, J.; Spranger, R.J.; Wullen, L.; Nilges, T. Fast Magnesium Conductiong Electrospun Solid Polymer Electrolyte. *Battery Supercap.* **2022**, *5*, e202200285. [[CrossRef](#)]
84. Reddy, M.J.; Chu, P.P. Ion pair formation and its effect in PEO:Mg solid polymer electrolyte system. *J. Power Sources* **2002**, *109*, 340–346. [[CrossRef](#)]
85. Basha, S.K.S.; Rao, M.C. Spectroscopic and electrochemical properties of PVP based polymer electrolyte films. *Polym. Bull.* **2018**, *75*, 3641–3666. [[CrossRef](#)]
86. Basha, S.K.S.; Sundari, G.S.; Kumar, K.V.; Rao, M.C. Preparation and dielectric properties of PVP-based polymer electrolyte films for solid-state battery application. *Polym. Bull.* **2018**, *75*, 925–945. [[CrossRef](#)]
87. Rathore, M.; Dalvi, A. Electrical characterization of PVA-MgSO₄ and PVA-Li₂SO₄ polymer salt composite electrolytes. *Mater. Today Proc.* **2019**, *10*, 106–111. [[CrossRef](#)]
88. Kalagi, S.S. Activation energy dependence on doping concentration in PVA-MgCl₂ composites. *Mater. Today Proc.* **2023**, *72*, 2691–2696.
89. Komal, B.; Yadav, M.; Kumar, M.; Tiwari, T.; Srivastava, N. Modifying potato starch by glutaraldehyde and MgCl₂ for developing an economical and environment-friendly electrolyte system. *e-Polymers* **2019**, *19*, 453–461. [[CrossRef](#)]
90. Tamilosai, R.; Palanisamy, P.N.; Selvasekarapandian, S.; Maheshwari, T. Solium alginate incorporated with magnesium nitrate as a novel solid biopolymer electrolyte for magnesium-ion batteries. *J. Mater. Sci. Mater. Electron.* **2021**, *32*, 22270–22285. [[CrossRef](#)]
91. Ismayl, J.K.; Hegde, S.; Vasachar, R.; Sanjeev, G. Novel solid biopolymer electrolyte based on methyl cellulose with enhanced ion transport properties. *J. Appl. Polym. Sci.* **2022**, *139*, 51826.
92. Buvaneshwari, P.; Mathavan, T.; Selvasekarapandian, S.; Krishna, M.V.; Naachiyan, R.M. Preparation and characterization of biopolymer electrolyte based on gellan gum with magnesium perchlorate for magnesium battery. *Ionics* **2022**, *28*, 3843–3854. [[CrossRef](#)]
93. Rajapaksha, H.G.N.; Perera, K.S.; Vidanapathirana, K.P. Characterization of a natural rubber based solid polymer electrolyte to be used for a magnesium rechargeable cell. *Polym. Bull.* **2022**, *79*, 4879–4890. [[CrossRef](#)]
94. Priya, S.S.; Karthika, M.; Selvasekarapandian, S.; Manjuladevi, R. Preparation and characterization of polymer electrolyte based on biopolymer I-Carrageen with magnesium nitrate. *Solid State Ion.* **2018**, *327*, 136–149. [[CrossRef](#)]
95. Ali, N.I.; Abidin, S.Z.Z.; Majid, S.R.; Jaafar, N.K. Role of Mg(NO₃)₂ as defective agent in ameliorating the electrical conductivity, structural and electrochemical properties of agarose-based polymer electrolytes. *Polymers* **2021**, *13*, 3357. [[CrossRef](#)] [[PubMed](#)]
96. Mahalakshmi, M.; Selvanayagam, S.; Selvasekarapandian, S.; Chandra, M.V.L.; Sangeetha, P.; Manjuladevi, R. Magnesium ion-conducting solid polymer electrolyte based on cellulose acetate with magnesium nitrate (Mg(NO₃)₂•6H₂O) for electrochemical studies. *Ionics* **2020**, *26*, 4553–4565. [[CrossRef](#)]

97. Sangeetha, P.; Selvakumari, T.M.; Selvasekarapandian, S.; Sri Kumar, S.R.; Manjukadevi, R.; Mahalakshmi, M. Preparation and characterization of biopolymer K-carrageenan with $MgCl_2$ and its application to electrochemical devices. *Ionics* **2020**, *26*, 233–244. [[CrossRef](#)]
98. Aziz, S.B.; Al-Zangana, S.; Woo, H.J.; Kadir, M.F.Z.; Abdullah, O.G. The compatibility of chitosan with divalent salts over monovalent salts for the preparation of solid polymer. *Results Phys.* **2018**, *11*, 826–836. [[CrossRef](#)]
99. Sangeetha, P.; Selvakumari, T.M.; Selvasekarapandian, S.; Mahalakshmi, M. Characterization of solid biopolymer electrolytes based on kappa-carrageenan with magnesium nitrate hexahydrate and its application to electrochemical devices. *Polym. Plast. Technol. Mater.* **2021**, *60*, 1317–1330.
100. Ismayil, J.K.; Hegde, S.; Sanjeev, G.; Murari, M.S. An insight into the suitability of magnesium ion-conducting biodegradable methyl cellulose solid polymer electrolyte film in energy storage devices. *J. Mater. Sci.* **2023**, *58*, 5389–5412.
101. Priya, S.S.; Karthika, M.; Selvasekarapandian, S.; Manjuladevi, R.; Monisha, S. Study of biopolymer I-carrageenan with magnesium perchlorate. *Ionics* **2018**, *24*, 3861–3875. [[CrossRef](#)]
102. Helen, P.A.; Perumal, P.; Sivaraj, P.; Diana, M.I.; Selvin, P.C. Mg-ion conducting electrolytes based on chitosan biopolymer host for the rechargeable Mg batteries. *Mater. Today Proc.* **2022**, *50*, 2668–2670. [[CrossRef](#)]
103. Kiruthika, S.; Malathi, M.; Selvasekarapandian, S.; Tamilarasan, K.; Moniha, V.; Manjuladevi, R. Eco-friendly biopolymer electrolyte, pectin with magnesium nitrate salt, for application in electrochemical devices. *J. Solid State Electrochem.* **2019**, *23*, 2181–2193. [[CrossRef](#)]
104. Kiruthika, S.; Malathi, M.; Selvasekarapandian, S.; Tamilarasan, K.; Maheshwari, T. Conducting biopolymer electrolyte based on pectin with magnesium chloride salt for magnesium battery application. *Polym. Bull.* **2020**, *77*, 6299–6317. [[CrossRef](#)]
105. Kayama, N.; Homma, K.; Yamakawa, Y.; Hirayama, M.; Kanno, R.; Yoneyama, M.; Kamiyama, T.; Kato, Y.; Hama, S.; Kawamoto, K.; et al. A lithium superionic conductor. *Nat. Mater.* **2011**, *10*, 682–686. [[CrossRef](#)] [[PubMed](#)]
106. Rathika, R.; Suthanthiraraj, S.A. Ionic interactions and dielectric relaxation of PEO/PVDF-Mg[$(CF_3SO_2)_2N_2$] blend electrolytes for magnesium ion rechargeable batteries. *Macromol. Res.* **2016**, *24*, 422–428. [[CrossRef](#)]
107. Shenbagavalli, S.; Muthuvinayagam, M.; Revathy, M.S. Electrical properties of Mg^{2+} ion-conductive PEO:P(PVdF-HFP) based solid blend polymer electrolytes. *Polymer* **2022**, *256*, 125242. [[CrossRef](#)]
108. Manjuladevi, R.; Thamilselvan, M.; Selvasekarapandian, S.; Mangalam, R.; Premalatha, M.; Monisha, S. Mg-ion conducting blend polymer electrolyte based on poly(vinyl alcohol)-poly(acrylonitrile) with magnesium perchlorate. *Solid State Ion.* **2017**, *308*, 90–100. [[CrossRef](#)]
109. Ponmani, S.; Prabhu, M.R. Development and study of solid polymer electrolytes based on PVdF-HFP/PVAc:Mg(ClO_4)₂ for Mg ion batteries. *J. Mater. Sci. Mater. Electron.* **2018**, *29*, 15086–15096. [[CrossRef](#)]
110. Polu, A.R.; Kumar, R.; Rhee, H.-W. Magnesium ion conducting solid polymer blend electrolyte based on biodegradable polymers and application in solid-state batteries. *Ionics* **2015**, *21*, 125–132. [[CrossRef](#)]
111. Manjuladevi, R.; Thamilselvan, M.; Selvasekarapandian, S.; Selvin, P.C.; Mangalam, R.; Monisha, S. Preparation and characterization of blend polymer electrolyte film based on poly(vinyl alcohol)-poly(aceylonitrile)/MgCl₂ for energy storage devices. *Ionics* **2018**, *24*, 1083–1095. [[CrossRef](#)]
112. Ponraj, T.; Ramalingam, A.; Selvasekarapandian, S.; Sri Kumar, S.R.; Manjuladevi, R. Mg-ion conducting triblock copolymer electrolyte based on poly(VdCl-co-AN-co-MMA) with magnesium nitrate. *Ionics* **2020**, *26*, 789–800. [[CrossRef](#)]
113. Hiraoka, K.; Inoue, M.; Takahashi, K.; Hayamizu, K.; Watanabe, M.; Seki, S. Analysis of ionic transport and electrode interfacial reaction, and NMR one-dimensional imaging of ther-based polymer electrolytes. *J. Electrochem. Soc.* **2021**, *168*, 060501. [[CrossRef](#)]
114. Park, B.; Andersson, R.; Pate, S.G.; Liu, J.; O'Brien, C.P.; Hernandez, G.; Mindemark, J.; Schaefer, J.L. Ion coordination and transport in magnesium polymer electrolytes based on polyester-co-polycarbonate. *Energy Mater. Adv.* **2021**, *2021*, 9895403. [[CrossRef](#)]
115. Manjuladevi, R.; Selvasekarapandian, S.; Thamilselvan, M.; Mangalam, R.; Monisha, S.; Selvin, P.C. A study on blend polymwe electrolyte based on poly(vinyl alcohol)-poly(acrylonitrile) with magnesium nitrate for magnesium battery. *Ionics* **2018**, *24*, 3493–3506. [[CrossRef](#)]
116. Ponmani, S.; Kalaiselvam, J.; Prabhu, M.R. Structural, electrical, and electrochemical properties of poly(vinylidene fluoride-co-hexafluoropropylene)/poly(vinyl acetate)-based polymer blend electrolytes for rechargeable magnesium ion batteries. *J. Solid State Electrochem.* **2018**, *22*, 2605–2615. [[CrossRef](#)]
117. Nayak, P.; Ismayil; Cyriac, V.; Hegde, S.; Sanjeev, G.; Murari, M.S.; Sudhakar, Y.N. Magnesium ion conducting free-standing biopolymer blend electrolyte films for electrochemical device application. *J. Non-Cryst. Solids* **2022**, *592*, 121741. [[CrossRef](#)]
118. Suvarna, K.; Kirubavathy, S.J.; Selvasekarapandian, S.; Krishna, M.V.; Ramaswamy, M. Corn silk extract-based solid-state biopolymer electrolyte and its application to electrochemical storage devices. *Ionics* **2022**, *28*, 1767–1782. [[CrossRef](#)]
119. Kanakaraj, T.M.; Bhajantri, R.F.; Chavan, C.; Cyriac, V.; Bulla, S.S.; Ismayil. Investigation on the structural and ion transport properties of magnesium salt doped HPMC-PVA based polymer blend for energy storage applications. *J. Non-Cryst. Solids* **2023**, *603*, 122276.
120. Koduru, H.K.; Marinov, Y.G.; Kaleemulla, S.; Rafailov, P.M.; Hadjichristov, G.B.; Scaramuzza, N. Fabrication and characterization of magnesium-ion-conducting flexible polymer electrolyte membranes based on a nanocomposite of poly(ethylene oxide) and potate starch nanocrystals. *J. Solid State Electrochem.* **2021**, *25*, 2409–2428. [[CrossRef](#)]

121. Kotobuki, M.; Kanamura, K. Fabrication of all-solid-state battery using $\text{Li}_5\text{La}_3\text{Ta}_2\text{O}_{12}$ Ceramic electrolyte. *Ceram. Int.* **2013**, *39*, 6481–6487. [CrossRef]
122. Aziz, A.A.; Tominaga, Y. Effect of Li salt addition on electrochemical properties of poly(ethylene carbonate)-Mg salt electrolytes. *Polym. J.* **2019**, *51*, 61–67. [CrossRef]
123. Perumal, P.; Abhilash, K.P.; Sivaraj, P.; Selvin, P.C. Study on Mg-ion conducting solid biopolymer electrolytes based on tamarind seed polysaccharide for magnesium ion batteries. *Mater. Res. Bull.* **2019**, *118*, 110490. [CrossRef]
124. Aziz, A.A.; Yominaga, Y. Magnesium ion-conductive poly(ethylene carbonate) electrolytes. *Ionics* **2018**, *24*, 3475–3481. [CrossRef]
125. Viviani, M.; Meereboer, N.L.; Saeaswati, N.L.P.A.; Loos, K.; Portale, G. Lithium and magnesium polymeric electrolytes prepared using poly(glycidyl ether)-based polymers with short grafted chains. *Polym. Chem.* **2020**, *11*, 2070–2079. [CrossRef]
126. Sarangika, H.N.M.; Dissanayake, M.A.K.L.; Senadeera, G.K.R.; Rathnayake, R.R.D.V.; Pitawala, H.M.J.C. Polyethylene oxide and ionic liquid-based solid polymer electrolyte for rechargeable magnesium batteries. *Ionics* **2017**, *23*, 2829–2835. [CrossRef]
127. Ge, X.; Song, F.; Du, A.; Zhang, Y.; Xie, B.; Huang, L.; Zhao, J.; Dong, S.; Zhou, X.; Cui, G. Robust self-standing single-ion polymer electrolytes enabling high-safety magnesium batteries at elevated temperature. *Adv. Energy Mater.* **2022**, *12*, 2201464. [CrossRef]
128. Gupta, A.; Jain, A.; Tripathi, S.K. Structural and electrochemical studies of bromide derived ionic liquid-based gel polymer electrolyte for energy storage. *J. Energy Storage* **2020**, *32*, 101723. [CrossRef]
129. Hambali, D.; Zainol, N.H.; Othman, L.; Isa, K.B.M.; Osman, Z. Magnesium ion-conducting gel polymer electrolytes based on poly(vinylidene chloride-co-acrylonitrile) (PVdC-co-AN): A comparative study between magnesium trifluoromethanesulfonate (MgTf_2) and magnesium bis(trifluoromethanesulfonimide) (Mg(TFSI)_2). *Ionics* **2019**, *25*, 1187–1198. [CrossRef]
130. Maheshwaran, C.; Mishra, K.; Kanchan, D.K.; Kumar, D. Mg^{2+} conducting polymer gel electrolytes: Physical and electrochemical investigations. *Ionics* **2020**, *26*, 2969–2980. [CrossRef]
131. Kotobuki, M.; Yan, B.; Lu, L. Recent progress on cathode materials for rechargeable magnesium batteries. *Energy Storage Mater.* **2023**, *54*, 227–253. [CrossRef]
132. Doe, R.E.; Han, R.; Hwang, J.; Gmitter, A.J.; Shterenberg, I.; Yoo, H.D.; Pour, N.; Aurbach, D. Novel electrolyte solutions comprising fully inorganic salts with high anodic stability for rechargeable magnesium batteries. *Chem. Comm.* **2014**, *50*, 243–245. [CrossRef]
133. Wang, T.; Zhao, X.; Liu, F.; Fan, L.-Z. Porous polymer electrolytes for long-cycle stable quasi-solid-state magnesium batteries. *J. Energy Chem.* **2021**, *59*, 608–614. [CrossRef]
134. Merrill, L.C.; Ford, H.O.; Scaefer, J.L. Application of single-ion conducting gel polymer electrolytes in magnesium batteries. *ACS Appl. Energy Mater.* **2019**, *2*, 6355–6363. [CrossRef]
135. Sheha, E.; Liu, F.; Wang, T.; Farrag, M.; Liu, J.; Yacout, N.; Kebebe, M.A.; Sharma, N.; Fan, L.-Z. Dual polymer/liquid electrolyte with BaTiO_3 electrode for magnesium batteries. *ACS Appl. Energy Mater.* **2020**, *3*, 5882–5892. [CrossRef]
136. Maheshwaran, C.; Kanchan, D.K.; Gohel, K.; Mishra, K.; Kumar, D. Effect of $\text{Mg}(\text{CF}_3\text{SO}_3)_2$ concentration on structural and electrochemical properties of ionic liquid incorporated polymer electrolyte membranes. *J. Solid State Electrochem.* **2020**, *24*, 655–665. [CrossRef]
137. Hambali, D.; Osman, Z.; Othman, L.; Isa, K.B.M.; Harudin, N. Magnesium (II) bis(trifluoromethanesulfonimide) doped PVdC-co-AN gel polymer electrolytes for rechargeable batteries. *J. Polym. Res.* **2020**, *27*, 159. [CrossRef]
138. Gupta, A.; Jain, A.; Tripathi, S.K. Structural, electrical and electrochemical studies of ionic liquid-based polymer gel electrolyte using magnesium salt for supercapacitor application. *J. Polym. Res.* **2021**, *28*, 235. [CrossRef]
139. Aziz, A.; Yoshimoto, N.; Yamabuki, K.; Tominaga, Y. Ion-conductive, thermal and electrochemical properties of poly(ethylene carbonate)-Mg electrolytes with glyme solution. *Chem. Lett.* **2018**, *47*, 1258–1261. [CrossRef]
140. Sharma, J.; Hashmi, S.A. Plastic crystal-incorporated magnesium ion conducting gel polymer electrolyte for battery application. *Bull. Mater. Sci.* **2018**, *41*, 147. [CrossRef]
141. Ponraj, T.; Tamalingam, A.; Selvasekaranpandian, S.; Srikumar, S.R.; Manjuladevi, R. Plasticized solid polymer electrolyte based on triblock copolymer polyvinylidene chloride-co-acrylonitrile-co-methyl methacrylate for magnesium ion batteries. *Polym. Bull.* **2021**, *78*, 35–57. [CrossRef]
142. Tominaga, Y.; Kato, S.; Nishimura, N. Preparation and electrochemical characterization of magnesium gel electrolytes based on crosslinked poly(tetrahydrofuran). *Polymer* **2021**, *224*, 123743. [CrossRef]
143. Hamsan, M.H.; Aziz, S.B.; Kadir, M.F.Z.; Brza, M.A.; Karim, W.O. The study of EDLC device fabricated from plasticized magnesium ion conducting chitosan based polymer electrolyte. *Polym. Test.* **2020**, *90*, 106714. [CrossRef]
144. Ponmami, S.; Prabhu, M.R. Sulfonate based ionic liquid incorporated polymer electrolytes for Magnesium secondary battery. *Polym. Plast. Technol. Eng.* **2019**, *58*, 978–991.
145. Nishino, H.; Liu, C.; Kanehashi, S.; Mayumi, K.; Tominaga, Y.; Shimomura, T.; Ito, K. Ionics transport and mechanical properties of slide-ring gel swollen with Mg-ion electrolytes. *Ionics* **2020**, *26*, 255–261. [CrossRef]
146. Singh, R.; Janakiraman, S.; Khalifa, M.; Anandhan, S.; Ghosh, S.; Venimadhav, A.; Biswas, K. An electroactive β -phase polyvinylidene fluoride as gel polymer electrolyte for magnesium-ion battery application. *J. Electroanal. Chem.* **2019**, *851*, 113417. [CrossRef]
147. Bhatt, P.J.; Pathak, N.; Mishra, K.; Kanchan, D.K.; Kumar, D. Effect of different cations on ion-transport behavior in polymer gel electrolytes intended for application in flexible electrochemical devices. *J. Electron. Mater.* **2022**, *51*, 1371–1384. [CrossRef]
148. Wang, L.; Li, Z.; Meng, Z.; Xiu, Y.; Dasari, B.; Zhao-Karger, Z.; Fichtner, M. Designing gel polymer electrolytes with synergistic properties for rechargeable magnesium batteries. *Energy Storage Mater.* **2022**, *48*, 155–163. [CrossRef]

149. Wang, J.; Zhao, Z.; Muchakayala, R.; Song, S. High-performance Mg-ion conducting poly(vinyl alcohol) membranes: Preparation, characterization and application in supercapacitors. *J. Membr. Sci.* **2018**, *555*, 280–289. [[CrossRef](#)]
150. Singh, R.; Janakiraman, S.; Agrawal, A.; Ghosh, S.; Venimadhav, A.; Biswas, K. An amorphous poly(vinylidene fluoride-co-hexafluoropropylene) based gel polymer electrolyte for magnesium ion battery. *J. Electroanal. Chem.* **2020**, *858*, 113788. [[CrossRef](#)]
151. Singh, R.; Janakiraman, S.; Khalifa, M.; Anandhan, S.; Ghosh, S.; Venimadhav, A.; Biswas, K. A high thermally stable polyacrylonitrile (PAN)-based gel polymer electrolyte for rechargeable Mg-ion battery. *J. Mater. Sci. Mater. Electron.* **2020**, *31*, 22912–22925. [[CrossRef](#)]
152. Maheshwaran, C.; Kanchan, D.K.; Mishra, K.; Kumar, D.; Gohel, K. Flexible, magnesium-ion conducting polymer electrolyte membrane: Mechanical, structural, thermal, and electrochemical impedance spectroscopic properties. *J. Mater. Sci. Mater. Electron.* **2020**, *31*, 15013–15027. [[CrossRef](#)]
153. Abdulwahid, R.T.; Aziz, S.B.; Brza, M.A.; Kadir, M.F.Z.; Karim, W.O.; Hamsan, H.M.; Asnawi, A.S.F.M.; Abdullah, R.M.; Nofal, M.M.; Dannoun, E.M.A. Electrochemical performance of polymer blend electrolytes based on chitosan: Dextran: Impedance, dielectric properties, and energy storage study. *J. Mater. Sci. Mater. Electron.* **2021**, *32*, 14846–14862. [[CrossRef](#)]
154. Ota, T.; Uchiyama, S.; Tsukada, K.; Moriya, M. Room-temperature Mg-ion conduction through molecular crystal $Mg(N(SO_2CF_3)_2)_2(CH_3OC_5H_9)_2$. *Front. Energy Res.* **2021**, *9*, 640777. [[CrossRef](#)]
155. Mori, S.; Obora, T.; Namaki, M.; Kondo, M.; Moriya, M. Organic crystalline solid electrolytes with high Mg-ion conductivity composed of nonflammable ionic liquid analogs and $Mg(TFSA)_2$. *Inorg. Chem.* **2022**, *61*, 7358–7364. [[CrossRef](#)] [[PubMed](#)]
156. Jayanthi, S.; Kalapriya, K. Structural, transport, morphological, and thermal studies of nano barium titanate-incorporated magnesium ion conducting solid polymer electrolytes. *Polym. Polym. Compos.* **2021**, *29*, S1158–S1167.
157. Wang, Y.; Wang, Z.; Zheng, F.; Sun, J.; Oh, J.A.S.; WU, T.; Chen, G.; Huang, Q.; Kotobuki, M.; Lu, L. Ferroelectric engineered electrode-composite polymer electrolyte interfaces for all-solid-state sodium metal battery. *Adv. Sci.* **2022**, *9*, 2105849. [[CrossRef](#)] [[PubMed](#)]
158. Jeyabalu, K.; Sundaramahalingam, K.; Devendran, P.; Manikandan, A.; Nallamuthu, N. Effect of electrical conductivity studied for CuS nanofillers mixed magnesium ion based PVA-PVP blend polymer solid electrolytes. *Phys. B Condensed Matter.* **2019**, *572*, 129–138. [[CrossRef](#)]
159. Jayalakshmi, K.; Ismayil; Hedge, S.; Ravindrachary, V.; Sanjeev, G.; Mazumdar, N.; Sindhoora, K.M.; Masti, K.; Jayalakshmi, S.P.; Murari, M.S. Methyl cellulose-based solid polymer electrolytes with dispersed zinc oxide nanoparticles: A promising candidate for battery applications. *J. Phys. Chem. Solids* **2023**, *173*, 111119. [[CrossRef](#)]
160. Nidhi, S.P.; Kumar, R. Synthesis and characterization of magnesium ion conductive in PVDF based nanocomposite polymer electrolytes disperse with MgO . *J. Alloys Compd.* **2019**, *789*, 6–14. [[CrossRef](#)]
161. Polu, A.; Kumar, R. Preparation and characterization of PEG-Mg(CH_3COO)₂-CeO₂ composite polymer electrolytes for battery application. *Bull. Mater. Sci.* **2014**, *37*, 309–314. [[CrossRef](#)]
162. Sarojini, S.; Padmapriya, L. Effect of size of the filler on the electrical conductivity of magnesium ion conducting polymer electrolyte. *Mater. Today Proc.* **2022**, *68*, 454–462. [[CrossRef](#)]
163. Helen, P.A.; Selvin, P.C.; Lashmi, D.; Diana, M.I. Amelioration of ionic conductivity (303K) with the supplement of MnO_2 filler in the chitosan biopolymer electrolyte for magnesium batteries. *Polym. Bull.* **2023**, *80*, 7715–7740. [[CrossRef](#)]
164. Maheshwaran, C.; Kanchan, D.K.; Mishra, K.; Kumar, D.; Gohel, K. Effect of active MgO nano-particles dispersion in small amount within magnesium-ion conducting polymer electrolyte matrix. *Nano-Struct. Nano-Objects* **2020**, *24*, 100587. [[CrossRef](#)]
165. Nidhi, S.P.; Kumar, R. Effect of Al_2O_3 on electrical properties of polymer electrolyte for electrochemical device application. *Mater. Today Proc.* **2021**, *46*, 2175–2178. [[CrossRef](#)]
166. Nidhi, S.P.; Kumar, R. Effect of nanoparticles on electrical properties of PVDF-based Mg^{2+} ion conducting polymer electrolytes. *Bull. Mater. Sci.* **2021**, *44*, 140. [[CrossRef](#)]
167. Sundar, M.; Selladurai, S. Effect of fillers on magnesium-poly(ethylene oxide) solid polymer electrolyte. *Ionics* **2006**, *12*, 281–286. [[CrossRef](#)]
168. Ponmani, S.; Selvakumar, K.; Prabhu, M.R. The effect of the geikeelite ($MgTiO_3$) nanofiller concentration in PVdF-HFP/PVAc-based polymer blend electrolytes for magnesium ion battery. *Ionics* **2020**, *26*, 2353–2369. [[CrossRef](#)]
169. Helen, P.A.; Ajith, K.; Diana, M.I.; Lakshmi, D.; Selvin, P.C. Chitosan based biopolymer electrolyte reinforced with V_2O_5 filler for magnesium batteries: An inclusive investigation. *J. Mater. Sci. Mater. Electron.* **2022**, *33*, 3925–3937. [[CrossRef](#)]
170. Mallikarjun, A.; Sangeetha, M.; Mettu, M.R.; Reddy, J.M.; Kumar, S.J.; Sreekanth, T.; Rao, V.S. Impedance spectroscopy and electrochemical cell studies of Mg^{2+} ion conducting with dispersed ZrO_2 nano filler in PVDF-HFP based nano composite solid polymer electrolytes. *Mater. Today Proc.* **2022**, *62*, 5204–5208. [[CrossRef](#)]
171. Patel, N.S.; Kumar, R. PVDF-HFP based nanocomposite polymer electrolytes for energy storage devices dispersed with various nano-fillers. *AIP Conf. Proc.* **2020**, *2220*, 080044.
172. Dannoun, E.M.A.; Aziz, S.B.; Brza, M.A.; Nofal, M.M.; Asnawi, A.S.F.M.; Yusof, Y.M.; Al-Zangana, S.; Hamsan, M.H.; Kadir, M.F.Z.; Woo, H.J. The study of plasticized solid polymer blend electrolytes based on natural polymers and their application for energy storage EDLC devices. *Polymers* **2020**, *12*, 2531. [[CrossRef](#)]
173. Sharma, J.; Hashmi, S. Magnesium ion-conducting gel polymer electrolyte nanocomposites: Effect of active and passive nanofillers. *Polym. Compos.* **2019**, *40*, 1295–1306. [[CrossRef](#)]

174. Song, S.; Kotobuki, M.; Zheng, F.; Li, Q.; Xu, C.; Wang, Y.; Li, W.D.Z.; Hu, N.; Lu, L. Communication-A composite polymer electrolyte for safer Mg batteries. *J. Electrochem. Soc.* **2017**, *164*, A741–A743. [[CrossRef](#)]
175. Aziz, S.B.; Dannoun, E.M.A.; Hamsan, M.H.; Abdulwahid, R.T.; Mishra, K.; Nofal, M.M.; Kadir, M.F.Z. Improving EDLC device performance constructed from plasticized magnesium ion conducting chitosan based polymer electrolytes via metal complex dispersion. *Membranes* **2021**, *11*, 289. [[CrossRef](#)] [[PubMed](#)]
176. Deivanayagam, R.; Cheng, M.; Wang, M.; Vasudevan, V.; Foroozan, T.; Medhekar, N.V.; Shahbazian-Yassar, R. Composite polymer electrolyte for highly cyclable room-temperature solid-state magnesium batteries. *ACS Appl. Energy Mater.* **2019**, *2*, 7980–7990. [[CrossRef](#)]
177. Sun, J.; Zou, Y.; Gao, S.; Shao, L.; Chen, C. Robust strategy of quasi-solid-state electrolytes to boost the stability and compatibility of Mg ion batteries. *ACS Appl. Mater. Interfaces* **2020**, *12*, 54711–54719. [[CrossRef](#)] [[PubMed](#)]
178. Wang, P.; Truck, J.; Hacker, J.; Schlosser, A.; Kuster, K.; Starke, U.; Reinders, L.; Buchmeiser, M.R. A design concept for halogen-free Mg^{2+}/Li^+ -dual salt-containing gel-polymer-electrolytes for rechargeable magnesium batteries. *Energy Storage Mater.* **2022**, *49*, 509–517. [[CrossRef](#)]
179. Luo, W.; Allen, M.; Raji, V.; Ji, X. An organic pigment as a high-performance cathode for sodium-ion batteries. *Adv. Energy Mater.* **2014**, *4*, 1400554. [[CrossRef](#)]
180. Chen, Y.; Luo, W.; Cater, M.; Zhou, L.; Dai, J.; Fu, K.; Lacey, S.; Li, T.; Wan, J.; Han, J.; et al. Organic electrode for non-aqueous potassium-ion batteries. *Nano Energy* **2015**, *18*, 205–211. [[CrossRef](#)]
181. Chen, Y.; Parent, L.R.; Shao, Y.; Wang, C.; Sprenkle, V.L.; Li, G.; Liu, J. Facile synthesis of chevrel phase nanocubes and their applications for multivalent energy storage. *Chem. Mater.* **2014**, *26*, 4904–4907. [[CrossRef](#)]
182. Mao, M.; Lin, Z.; Tong, Y.; Yue, J.; Zhao, C.; Lu, J.; Zhang, Q.; Gu, L.; Suo, L.; Hu, Y.S.; et al. Iodine vapor transport-triggered preferential growth of chevrel Mo_6S_8 nanosheets for advanced multivalent batteries. *ACS Nano* **2020**, *14*, 1102–1110. [[CrossRef](#)] [[PubMed](#)]

Disclaimer/Publisher’s Note: The statements, opinions and data contained in all publications are solely those of the individual author(s) and contributor(s) and not of MDPI and/or the editor(s). MDPI and/or the editor(s) disclaim responsibility for any injury to people or property resulting from any ideas, methods, instructions or products referred to in the content.